THE UNIVERSITY OF ALBERTA

"THE DESIGN OF A SPECIAL PURPOSE NONLINEAR CONTROLLER"

by

N.L. Arrison

A THESIS

SUBMITTED TO THE FACULTY OF GRADUATE STUDIES

IN PARTIAL FULFILMENT OF THE REQUIREMENTS FOR THE

DEGREE OF MASTER OF SCIENCE

IN CHEMICAL ENGINEERING

DEPARTMENT OF CHEMICAL AND PETROLEUM ENGINEERING

EDMONTON, ALBERTA

OCTOBER, 1965

THE UNIVERSITY OF ALBERTA

FACULTY OF GRADUATE STUDIES

The undersigned certify that they have read, and recommend to the Faculty of Graduate Studies for acceptance, a thesis entitled "The Design of a Special Purpose Nonlinear Controller" submitted by N.L. Arrison, B.Sc. in partial fulfilment of the requirements for the Degree of Master of Science in Chemical Engineering.

Acknowledgements

The author wishes to express his sincere appreciation of the helpful guidance given by Dr. R.A. Ritter, under whose supervision this investigation was performed.

The financial support of the National Research Council and of the Canadian Kodak Company Limited is gratefully acknowledged.

Abstract

In many chemical engineering control problems the amount of movement of the manipulated variable is as important as that of the controlled variable. In this study such a case was examined. The system investigated was one in which the controlled variable had to only stay within limits. The distance between the limits was then used to lower the fluctuations, root-mean-square, of the manipulated variable. A study of nonlinear controllers was carried out to see if the root-mean-square could be lowered while still preserving a rapid and highly damped start-up response or mathematically a low value of the integral with respect to time of the absolute value of the manipulated variable times time. Using a statistical describing function approach for analytical root-mean-square calculations and an analogue computer, different continuous nonlinearities were investigated. The nonlinearity with the best root-mean-square and above integral values, in the author's opinion, is one in which a simply proportional controller has its input changed from a linear error to $|(\text{error})| \times (\text{error})$ and the gain of the proportional controller itself is lowered.

Table of Contents

List of Figures

Nomenclature

A	area $(\text{length})^2$
e	error, (length)
E_{ms}	mean-square of error $(\text{length})^2$
E_{rms}	root-mean-square of error (length)
h	liquid level of tank (length)
h_{ms}	mean-square of liquid level $(\text{length})^2$
h_{rms}	root-mean-square of liquid level (length)
H_σ	statistical describing function (length/length)
K	gain
K_2	1/area $(1/\text{length}^2)$
$f(v)$	probability density (1/length)
q_o	flow out (manipulated variable) $(\text{length})^3/\text{sec.}$
q_1	flow in (load variable) $(\text{length})^3/\text{sec.}$
r	reference (length)
t	time (seconds)
v	any fluctuating variable (length)
$\phi_v(\omega)$	power spectral density of v $(\text{length})^2(\text{seconds})$
$\phi_x(\omega)$	power spectral density of x $(\text{length})^2(\text{seconds})$

Symbols for Laplace Transforms of Variables

E	Laplace transform of e
$h(s)$	Laplace transform of h
Q	Laplace transform of q_o
Q_s	Laplace transform of q_1

Introduction

The theory of linear control is well developed. If a system and its controller are linear, one needs only adjust the proportional, reset, or rate constants to obtain whatever criterion was specified such as minimum area, stability, etc. Once a criterion has been found it can be transferred to related systems with ease. However, few systems in practice are truly linear. Also, in many cases, it is possible to design a nonlinear controller that will yield a better response than a linear controller. As a result, nonlinear control theory has been in much demand.

Using nonlinear control theory, it is generally possible to design a better controller for two reasons. First, instead of replacing the nonlinearity with an approximate linear expression or assuming it does not exist, the nonlinearity can be studied for its true effect on the closed loop. Second, one can then design the nonlinear controller to compensate or use nonlinearities to obtain the best possible response. Thus, it might be said that nonlinear control theory gives one the power to tailor each controller more closely to a system's particular needs.

Nonlinear control theory has been slow in general acceptance because of the difficulty normally encountered in obtaining an analytical solution to a control problem. For up to the present time, there is no general analytical approach

to all nonlinear problems. Instead, there are certain types of approximations, such as the describing function approach to stability analysis or statistical describing function for rms (root-mean-square) calculations as used in the present study; and then there are special approaches, such as the phase plane technique which is used to check the response of second order systems. If the feedback loops and nonlinearities become numerous, an analytical solution quickly becomes impractical if not impossible. When this occurs a solution is obtained by using the computer, either digital or analogue.

With the above thoughts in mind, this study designs a nonlinear controller. The problem is such that it is desired to keep the controlled variable within limits, only, while keeping the manipulated variable from fluctuating as much as possible. Also, the controlled variable must not feel large upsets for long. To explain this more fully, consider the reboiler on a distillation column. Here, it is desired to keep the liquid level in the reboiler above the steam tubes and a given distance below the bottom plate. At the same time variations in the outflow must be minimized so as not to disturb downstream processes. Also, sudden load disturbances such as occur during start-up should damp out quickly. This problem will be investigated throughout the remainder of this study.

One must now translate the above statements of desired response into definite mathematical criteria. After the criteria are chosen an order of priority must then be established.

Both of these decisions are dependent on the designer's judgement. The criteria that guided the outcome of this study are listed below in order of priority as follows:

1) Stability

2) The lowest value of ITAM($\int |q_o| t dt$) for step changes in the liquid level (q_o = manipulated variable, t = time)

3) The lowest rms (root-mean-square) value for the manipulated variable for a random Gaussian load change.

Continuous functions are studied to meet the above demands.

Literature Review

The following short summaries and reviews represent the literature covering the subject of this study. The first paper is one showing how this problem can be handled in the design stage. The second paper describes a commercial controller that is used to smooth out flows from tanks. In the last part of this summary and review a discussion is presented of other controllers and theory in general.

R. Jackson(5) suggests that the object of all controllers is to maintain some measured quantity y(t) close to Y, in spite of a disturbance i(t). He then mentions that the following work arose because it was felt that a lack of information at the design stage should not lead to complete impotence. Rather, the system should be over designed based on a safety factor that is related to the designer's ignorance of the system.

Jackson then points out that at the design stage the maximum values of quantities and rates are generally known; and he then goes on to state the basic mathematical problem as follows: "In a stable linear filter the output y(t) at time t is related to values of the input i(t) at all previous times by an equation of form

$$y(t) = \int_0^{\infty} W(u)\, i(t - u)\, du \qquad (1)$$

where the weighting function W(u) characterizes the particular

system considered and the stability conditions demand that $\int_0^\infty |W(u)|du$ should exist. It is assumed that i(t) is uniformly bounded and that the origin for i(t) is chosen so that

$$|i(t)| \leqslant i_m \qquad \text{(all } t) \qquad (2)$$

It is also assumed that the rate of change of i(t) is uniformly bounded or, slightly more generally, that

$$\frac{|i(t_1) - i(t_2)|}{|t_1 - t_2|} \leqslant i'_m \qquad (\text{all } t_1, t_2) \qquad (3)$$

The problem is then to find the corresponding smallest bound y_m such that $|Y(t)| \leqslant y_m$ for all t."( ) A procedure is then developed for constructing that i(t) which makes y, at some specified time, as large as possible. The value of $y (= y_m)$ can then be obtained from equation (1). The solution to this problem can be found when the performance is specified by limits $\pm y_m$ and when the information available about the disturbance is of the form specified by equations (2) and (3).

Jackson then proceeds to develop the mathematical theory for solution in a rigorous manner. Having formally proved his method, he then applies his procedure to the practical application of level control systems. He divides the types of level control into three classes called flow smoothing, level control, and given valve motor.

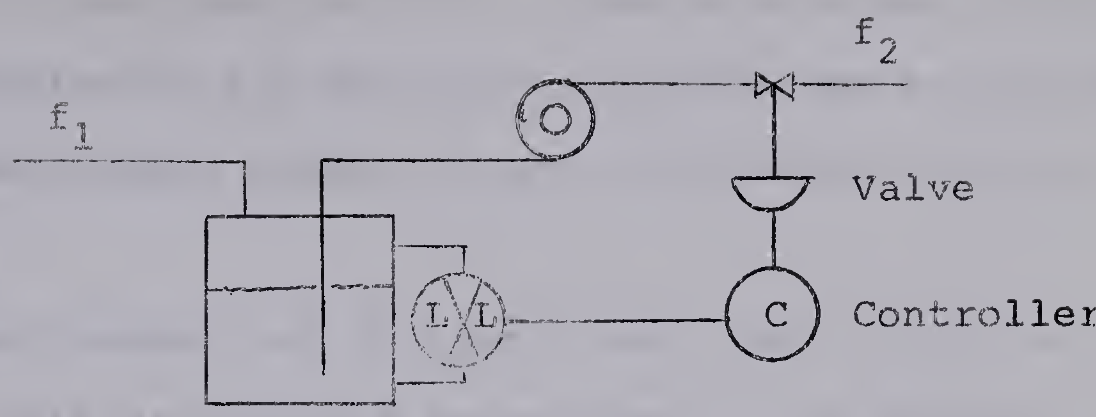

Figure 1

The flow smoothing system, as described by Jackson, makes use of the available free space in the vessel to smooth out fluctuations in the out flow f_2 (see Figure 1). The aim here is to vary f_2 as slowly as possible while still checking the level variations before they overflow or empty the tank. Jackson states the object of design is to predict:

1. The minimum size of vessel which can be used if the desired smoothness of the controlled flow is to be obtained without any possibility of the vessel overflowing or emptying.

2. Size and speed requirements for the control valves regulating the flow f_2.

With the level control system, it is desired to keep the liquid level between narrow limits. Here the vessel size is assumed given and the designer must specify a valve of adequate speed and size. The third control class, given valve motor, is the reverse problem of the level control system.

All the above control problems are basically the same.

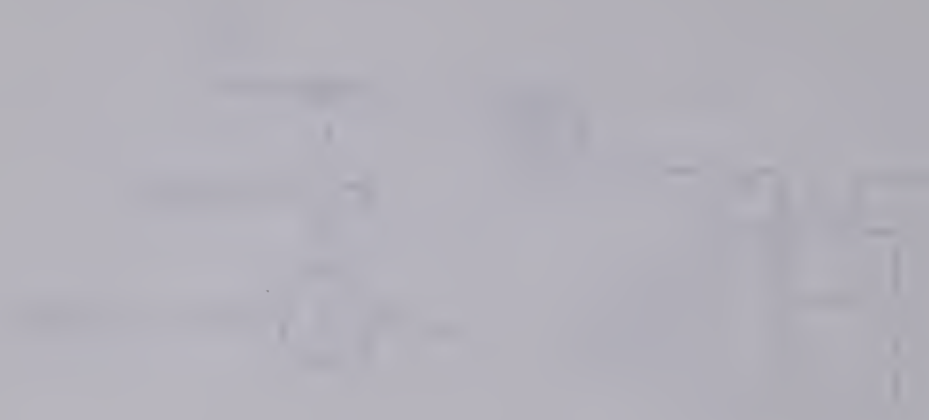

Thus, assuming proportional control, Jackson develops graphs so that the solution to all the above problems can be obtained without the considerable amount of work that would otherwise be needed.

This short summary of Jackson's work thus shows how the problem of this study could be handled in the design stage.

Existing Controller

Foxboro Company has developed a nonlinear tool which makes a dead zone around the reference to help smooth out the flow( ). This device is used in conjunction with a proportional or proportional-reset controller.

There is no question that a controller with a dead zone will most efficiently lower the rms of the manipulated variable if the dead zone is made relatively large. Should there be an upset, however, would this controller be able to handle it? Can it handle start-up? The answer to these questions and the related ones of relative stability and damping properties can best be answered by remembering the phase plane diagram of a second order system with a dead zone. On the phase plane the dead zone is seen to be a hinderance to damping for step inputs. The larger the dead zone the greater the hinderance. Since it is desired to have both the ability to damp out sudden changes and to lower the rms, this type of controller can be improved upon.

The great advantage of this controller is its versatility for it is used in many applications besides the above-mentioned one.

General Theory

O.J.M. Smith has considered many control devices. One which was of interest was posicast control(7). This is because posicast control makes the manipulated variable react swiftly to step changes in the controlled variable and does not let the system fluctuate in the ideal use. However, this control is of little value here for two reasons. One is that it is limited to underdamped systems. Two, the rms of the manipulated variable would be much too high if it responded to each fluctuation of the controlled variable.

O.J.M. Smith has covered much nonlinear control theory in general(7). In one section, he shows how to use the phase plane for the design of servo control. While illustrating his method with an example problem, he uses the |(variable|x (variable) expression used in this study as $e|e|$.

Brown and Nilsson( ) give an excellent introduction into the use of random signals as applied to linear systems. Thaler and Pastel( ) advance the discussion of the use of random signals to nonlinear systems; and it is their methods together with those presented by Gibson(4) which are used in this study.

Theory

In the theoretical development a mathematical model for the process dynamics is first obtained. A control loop is then established and the reasons for a given filter and for discarding certain nonlinearities are given. A stability analysis is then carried out on both the linear and nonlinear systems. Finally, a short mathematical development is given of Thaler and Pastel's(9) method of obtaining rms values in linear and nonlinear systems that have been excited by random load fluctuations. The author then extends the method to study the response to random disturbances of the manipulated variable as well as the controlled variable.

The mathematical model is developed using Figure 2.

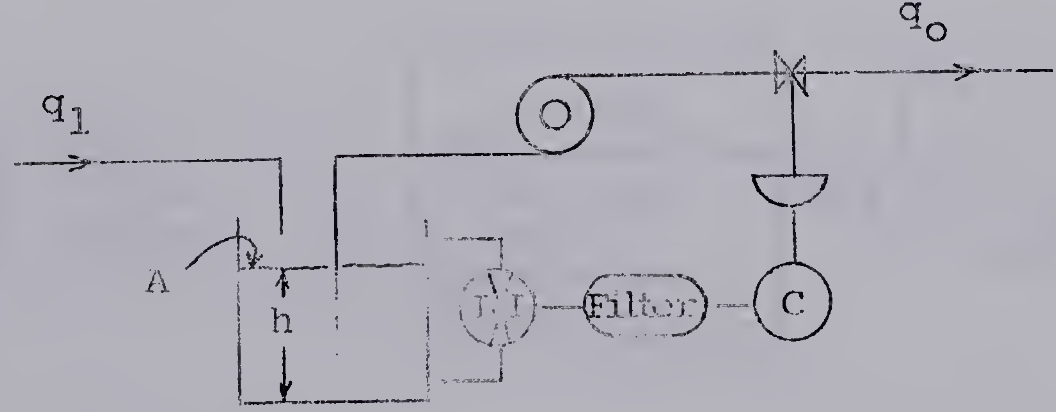

Figure 2

Writing a material balance

$$A \frac{dh}{dt} = q_1 - q_o$$

A = tank area

t = time

h = liquid level

q_1 = flow in

q_o = flow out

The Laplace transform of this equation may be written

$$A\ S\ h(S) = L[q_1] - L[q_o]$$

$$h(S) = \frac{L[q_1]}{A\ S} - \frac{L[q_o]}{A\ S}$$

provided that $h[0^+]$ is assumed equal to zero. A capacitance element thus describes the dynamic response of the process. The control loop is now closed giving the block diagram of Figure 3.

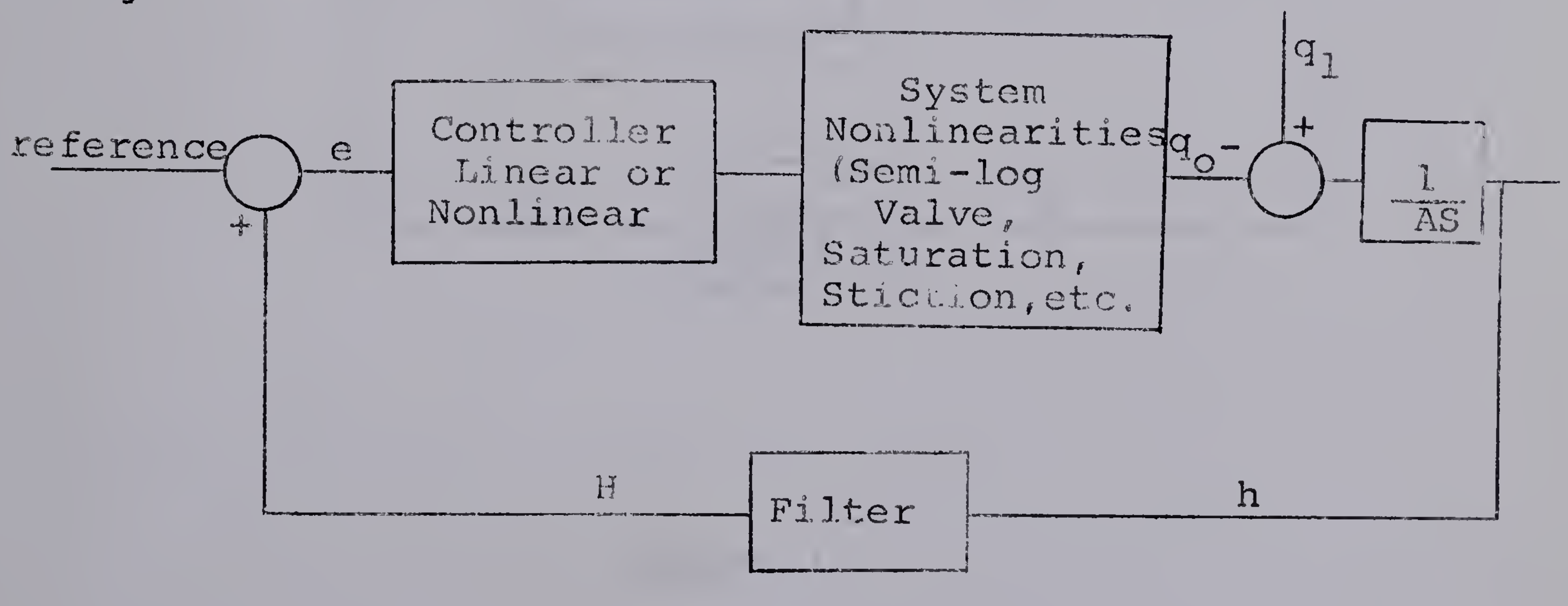

Figure 3

The selection of a filter is arbitrary. However, a first order filter with a time constant of 0.1 of A will remove unwanted high frequencies in the feedback signal; yet, it will not seriously interfere with the response of the system. Thus, the transfer function of the filter is $\frac{1}{T_F S + 1}$ where $T_F = 0.1A$.

It is intended to operate the system within its flow limits; therefore, the nonlinearity, saturation of the valve output, is dropped from the model. The semi-log valve characteristic is also neglected. This is because the nonlinearity is minimized by the pressure drop relationship between the valve and the pipe as the flow changes. Other nonlinearities, such as, stiction in the valves are neglected because of the very small effect they have on the process. For the reasons given above the block diagram of Figure 3 can simplified to that of Figure 4.

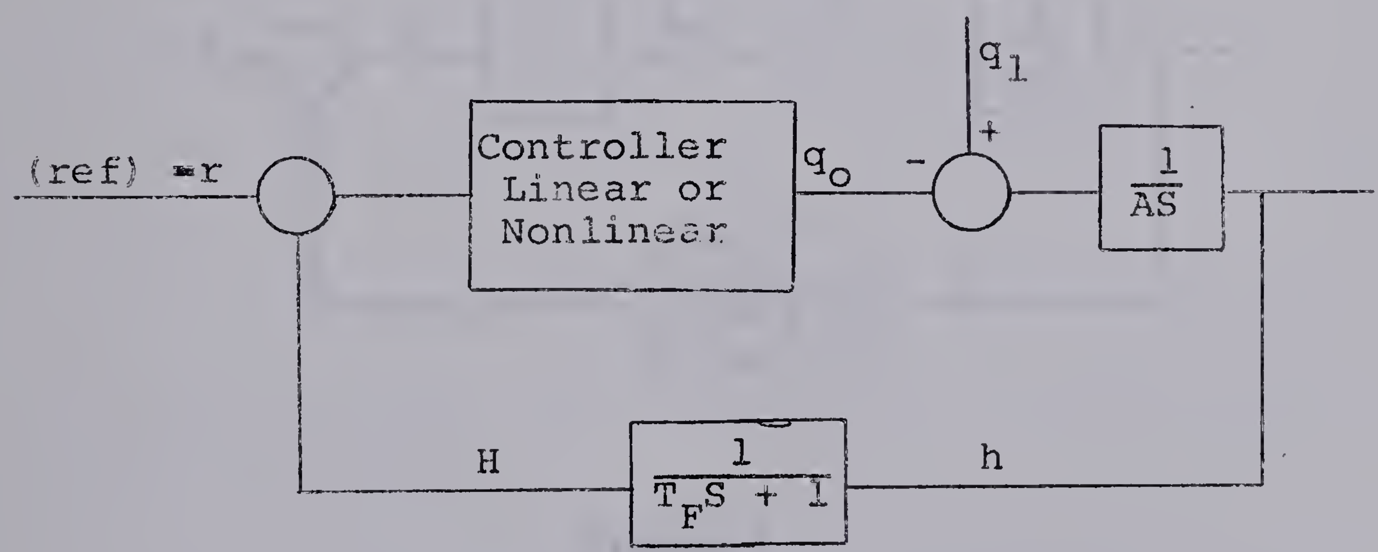

Figure 4

The block diagram of Figure 4 represents the system studied in this work. At this stage, the author would like to emphasize the fact that the controlled variable h has only to stay within limits. It is then intended to use the region between these limits to damp out fluctuations in the manipulated variable q_o. Also, it is desired that the ITAM ($\int |q_o| tdt$) be small for large steps because of start-up and possible large upsets.

Stability Studies

If linear control is used on the system of Figure 4, it is found, by computer, that a simple proportional element with a gain of four gives the lowest ITAM value. For these conditions, the block diagram is that of Figure 5.

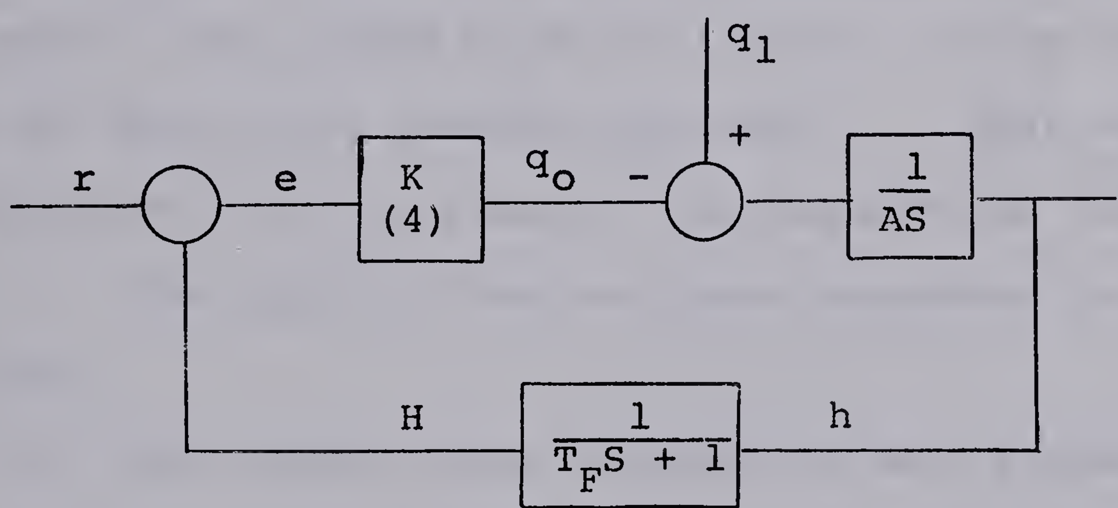

Figure 5

The Root Locus plot of the characteristic equation of Figure 5 is shown in Figure 6.

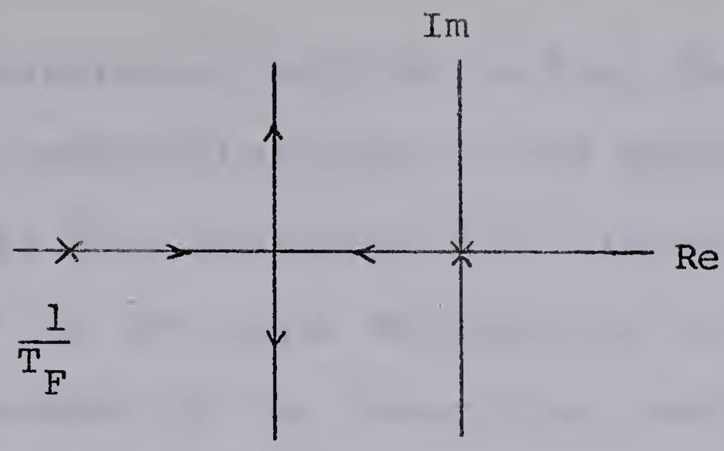

Root Locus plot of characteristic equation: $\frac{1}{A\,S(T_F S + 1)} = \frac{-1}{K}$

Figure 6

Because no roots lie in the right-half-plane the linear system is stable for all gains. Note, however, that as the gain increases the system becomes more oscillatory.

A study of the stability of the nonlinear functions $e|e|$ and e^3 that proved to be of interest is now carried out using the describing function approach(9). This method is an approximation which is based on the assumptions that:

1) The input to the nonlinear component is a pure sine wave.

2) The output curve contains no zero frequency component and no subharmonic terms, and all higher harmonic terms may be discarded.

A procedure suggested when using this method is as follows:

1) Isolate the nonlinear component in the block diagram.

2) Develop a Fourier series representation of the nonlinearity based on the above assumptions.

3) The describing function is then the ratio of the magnitude of the fundamental term in the Fourier series for the output wave to the magnitude of the input sinusoid at a phase angle which is the angle between the two sine waves.

4) The product of the describing function and the linear characteristic equation is then studied in the normal fashion for stability. (When the describing function is frequency dependent, a new Root Locus plot etc. must be constructed for each frequency.)

In mathematical notation, if the input wave is designated by

$$\text{Input} = E \sin wt$$

and the fundamental frequency term in the Fourier series for the output is designated by

$$\text{Fundamental output term} = F(E,w) \sin \left[wt + \phi(E,w)\right]$$

then the describing function for the nonlinear component is defined to be

$$\text{Describing function} = G_D(E,jw) = \left|\frac{F(E,w)}{E}\right| \angle \phi(E,w)$$

The above method is now applied to the system of Figure 4 which has, first, a nonlinear controller with a $K\,e|e|$ characteristic and, second, a controller with a $K\,e^3$ characteristic. Letting $g(e) = e|e|$ or e^3 and g( ) equal the mathematical operations |variable| x variable and $(\text{variable})^3$, the block diagram becomes that of Figure 7.

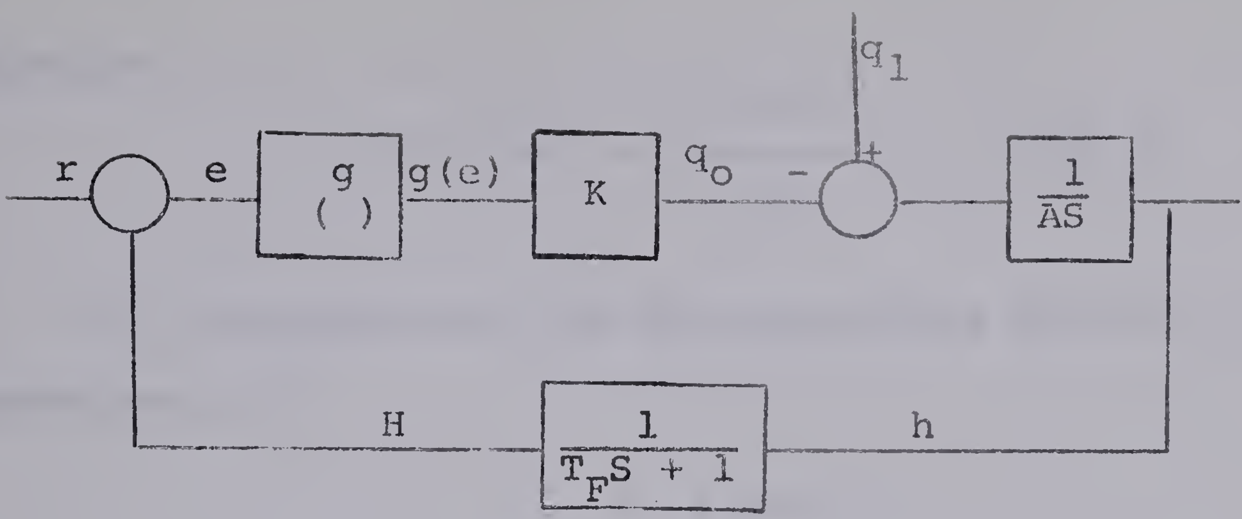

Figure 7

The nonlinearities are already isolated in this case. Therefore, the Fourier series and describing functions are easily obtained for the two nonlinearities as outlined in the above procedure.

a) Calculations for the describing function of the nonlinearity $e|e|$

$$e = E \sin wt$$

$$e|e| = E^2 \sin wt|\sin wt|$$

The two constants for the fundamental frequency in the Fourier series are:

$$A_1 = \frac{2}{\pi} \int_0^\pi E^2 \sin^2 wt \cos wt \, dwt$$

$$= 0$$

Note: $\sin wt = \sin wt$ from 0 to π

$$B_1 = \frac{2}{\pi} \int_0^\pi E^2 \sin^3 wt \, dwt$$

$$= \frac{4E^2}{3\pi} = 0.425 \, E^2$$

Therefore

$$G_D(E,jw) = \frac{0.425E^2}{E} = 0.425\ E$$

b) Calculations for the describing function of the nonlinearity e^3

$$e = E \sin wt$$

$$e^3 = E^3 \sin^3 wt$$

Again the Fourier series constants are:

$$A_1 = \frac{2}{\pi} \int_0^{\pi} E^3 \sin^3 wt \cos wt \, dwt$$

$$= 0$$

$$B_1 = \frac{2}{\pi} \int_0^{\pi} E^3 \sin^4 wt \, dwt$$

$$= \frac{3}{4} E^3$$

Therefore

$$G_D(E,jw) = 0.75 \frac{E^3}{E} = 0.75\ E$$

The calculations done in a) and b) above show that the describing function for both $e|e|$ and e^3 are only amplitude dependent. Thus, on applying step 4 of the suggested procedure, it can be seen that both nonlinear systems are stable because the linear system is stable for all gains.

Root-Mean-Square (rms) Calculations

The theory is first presented for the mean-square (ms) calculations in the frequency domain for any random variable v. Second, a method is discussed that uses a statistical describing function to deal with nonlinearities when the system is under random load fluctuations. Third, the theory behind the statistical describing function is stated. Fourth, the above methods of calculating the rms are applied to the controlled variable h. Fifth, the author extends the rms calculations to the manipulated variable q_o. Sixth, the author predicts approximately the effect given nonlinearities will have on both h and q_o rms values.

A random variable which has been described in terms of its time variation may also be described in terms of its frequency spectrum. The following thus develops a relationship between the mean-square (ms) value of a random variable and its frequency content.

"A convenient starting point is the time equation for the ms value which is

$$v_{ms} = \lim_{T\to\infty} \frac{1}{2T} \int_{-T}^{T} \left[v(t)\right]^2 dt \qquad (1)$$

v = variable, T = time limit, t = time

There are obvious mathematical advantages available if one or both of the variable functions v(t) in equation (1) can be replaced by their Fourier transforms. Unfortunately, this

cannot be done directly since the Fourier integral of a random time function does not converge. However, if a new function $v_T(t)$ is defined, the desired manipulation may be made. The function $v_T(t)$ is defined to exist only in the time interval $-T < t < T$, being exactly the same as $v(t)$ during this interval but being zero outside the interval. With this definition (1) may be rewritten

$$v_{ms} = \lim_{T\to\infty} \frac{1}{2T} \int_{-T}^{T} \left[v_T(t)\right]^2 dt \tag{2}$$

The Fourier transform of the variable $v_T(t)$ exists

$$v_T(t) = \frac{1}{2\pi} \int_{-\infty}^{\infty} V_T(w)\, e^{jwt}\, dw \tag{3}$$

Substituting (3) in (2) for only one factor of $v_T(t)$

$$v_{ms} = \lim_{T\to\infty} \frac{1}{2T} \int_{-T}^{T} v_T(t) \left[\frac{1}{2\pi} \int_{-\infty}^{\infty} V_T(w)\, e^{jwt}\, dw\right] dt \tag{4}$$

Changing the order of integration

$$v_{ms} = \frac{1}{2\pi} \int_{-\infty}^{\infty} V_T(w) \left[\lim_{T\to\infty} \frac{1}{2T} \int_{-T}^{T} v_T(t)\, e^{jwt}\, dt\right] dw \tag{5}$$

but

$$V_T(w) = \int_{-\infty}^{\infty} v_T(t)\, e^{-jwt}\, dt \tag{6}$$

Therefore, in equation (6) it is seen that

$$V_T(-w) = \lim_{T\to\infty} \int_{-T}^{T} v_T(t)\, e^{jwt}\, dt \tag{7}$$

Thus equation (5) may be rewritten

$$v_{ms} = \frac{1}{2\pi} \int_{-\infty}^{\infty} \lim_{T\to\infty} \frac{1}{2T} \left[V_T(w)\ V_T(-w)\right] dw \qquad (8)$$

From equation (8) the power spectral density is defined as

$$\phi_v(w) = \lim_{T\to\infty} \frac{1}{2T} \left[V_T(w)\ V_T(-w)\right] \qquad (9)$$

It is readily seen that equation (8) approaches equation (2) as $T\to\infty$. Hence, the desired relationship between the mean-square (ms) value of the random variable and its frequency content is(4)"

$$v_{ms} = \frac{1}{2\pi} \int_{-\infty}^{\infty} \phi_v(w)\ dw \qquad (10)$$

The power spectral density function equation (9) is simply the Fourier transform of the autocorrelation function(5). The autocorrelation function is the equation describing the statistical behavior of the variable v.

If x(t) is a time-stationary random function with a known autocorrelation function (or power spectral density) and the poles of Y(S), in Figure 8, lie in the left-half plane then(5)

$$\phi_v(w) = \phi_x(w)\ |Y(jw)|^2 \qquad (11)$$

where $\phi_x(w)$ = power spectral density of variable x

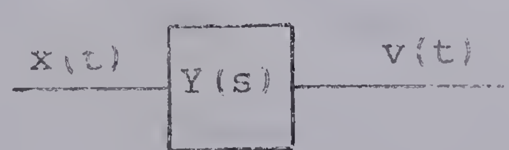

Figure 8

(The above statement is proven in reference 1.) This completes the development required to obtain ms and thus rms values for linear systems.

The ms values for nonlinear systems are calculated in a similar manner. The nonlinearity is simply replaced by the term H_σ called the statistical describing function and the calculations are then carried out as explained above. The result for v_{ms} then contains the term H_σ. H_σ is then eliminated by obtaining it as a function of v and solving the equation for v either analytically or graphically.

It now remains to be shown that the statistical describing function H_σ can be calculated as a function of v. First, it is assumed that the load fluctuations and all other variables in the control loop including v, have a Gaussian probability density. (The validity of this assumption is discussed in reference 9.) In this study the average value of all variables in the control loop are taken as zero. Therefore, the probability function has the shape shown in Figure 9

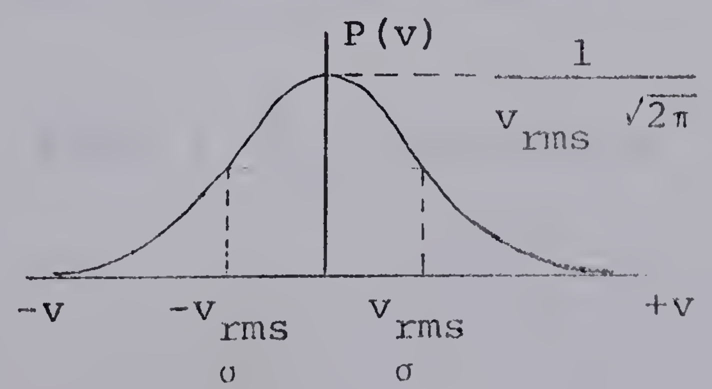

Figure 9

and is expressed mathematically as

$$\text{Probability density of } v = P(v) = \frac{e^{-\frac{v^2}{2\sigma^2}}}{\sigma\sqrt{2\pi}} \tag{12}$$

where

$$\sigma = \text{standard deviation of } v$$

When the probability density is known, the average value of the random signal is by definition

$$v_{av} = \int_{-\infty}^{\infty} v\, P\,(v)\, dv \tag{14}$$

and similarly, the mean-square (ms) value is

$$v_{ms} = \int_{-\infty}^{\infty} v^2\, P(v)\, dv \tag{15}$$

Also, if instead of v^2 in Equation (15), we have some other function $f(v)$; then its average value $\overline{f(v)}$ is given by:

$$\overline{f(v)} = \int_{-\infty}^{\infty} f(v)\, P(v)\, dv \tag{16}$$

Equation (16) now makes it possible to calculate the statistical describing function H_σ. If for the nonlinear element, the function f(v) is set equal to the square of the output and v_{ms} is the square of the input H_σ becomes:

$$H_\sigma = \sqrt{\frac{\overline{f(v)}}{v_{ms}}} \tag{17}$$

Thus, the statistical describing function is equal to the square root of the average mean square of the output over input for any nonlinear element.

The above theory is now applied to the systems shown in Figures 5 and 7. When talking of a statistical describing function, the linear system in Figure 5 merely becomes a special case of that shown in Figure 7. Therefore, it is necessary to consider only the nonlinear system of Figure 7.

Let

H_σ = statistical describing function of nonlinearities

$E(s) = L[e]$

$h_f(s) = L[H]$

$h(s) = L[h]$

$Q(s) = L[q_o]$

$Q_D(s) = L[q_1]$

$K_2 = \frac{1}{A}$

The new block diagram for the nonlinear system is shown in Figure 10.

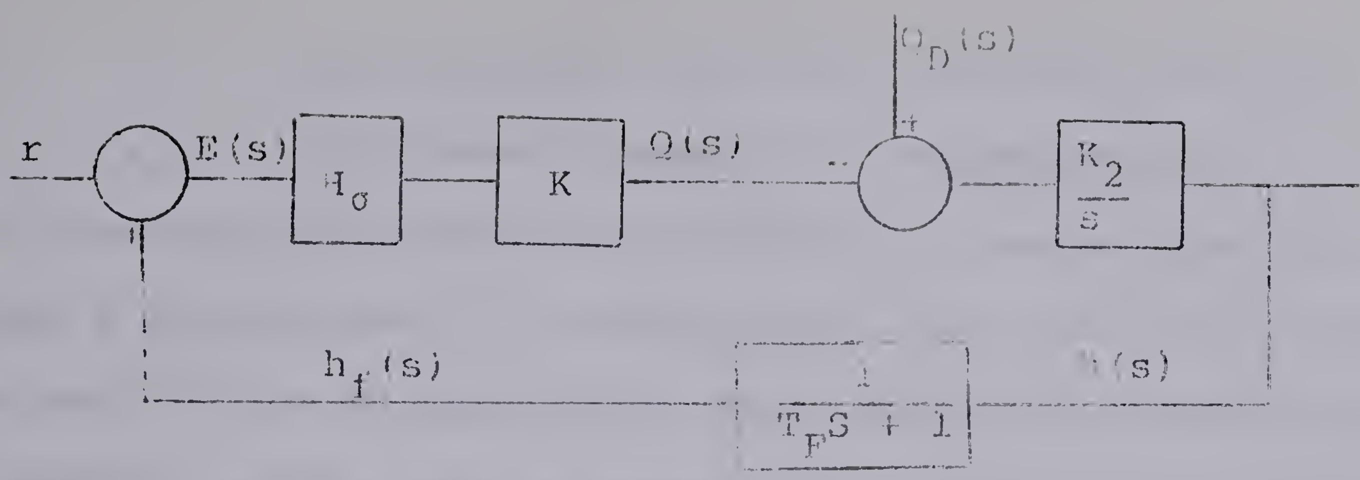

Figure 10

$Q_D(S)$ is the Laplace transform of the time equation (intercorrelation) describing the Gaussian random movement of the load variable. For the mathematical model on the computer, $Q_D(S)$ was obtained from a Gaussian random generator which passed its output through a low frequency filter with the Laplace transform $\left(\frac{S}{10S + 1}\right)$. The Gaussian random generator has a high requency filter with the Laplace transform $\left(\frac{1}{0.0159S + 1}\right)$[3] However, this filter can be neglected for simplicity. This is because the filter in the feedback of the control loop, for practical purposes, eliminates all high frequencies. Its Laplace transform is $\left(\frac{1}{0.5S + 1}\right)$ on the time scaled computer model. Thus, before the filter on the random generator has any effect, the high frequencies have been reduced at least one order of magnitude by the feedback loop filter.

The Gaussian random generator output can be represented by the Laplace transform $\frac{nw_o}{S + w_o}$ where:

n = low frequency magnitude of noise spectrum

w_o = half-power frequency of noise spectrum

If the frequency output of the Gaussian random generator varied from 0 radians/sec to ∞ radians/sec, the value of w_o would be one. Since neglecting the high frequency filter on the generator is the same as assuming the frequencies go to ∞, the value of w_o is taken as one. (In all the following calculations one may note that they are not highly sensitive to changes in w_o values as the power of w_o is the same in both numerator and denominator.) To obtain the value of n in the Laplace transform representation of the Gaussian random generator output, consider the new block diagram of the mathematical model used on the computer (see Figure 11).

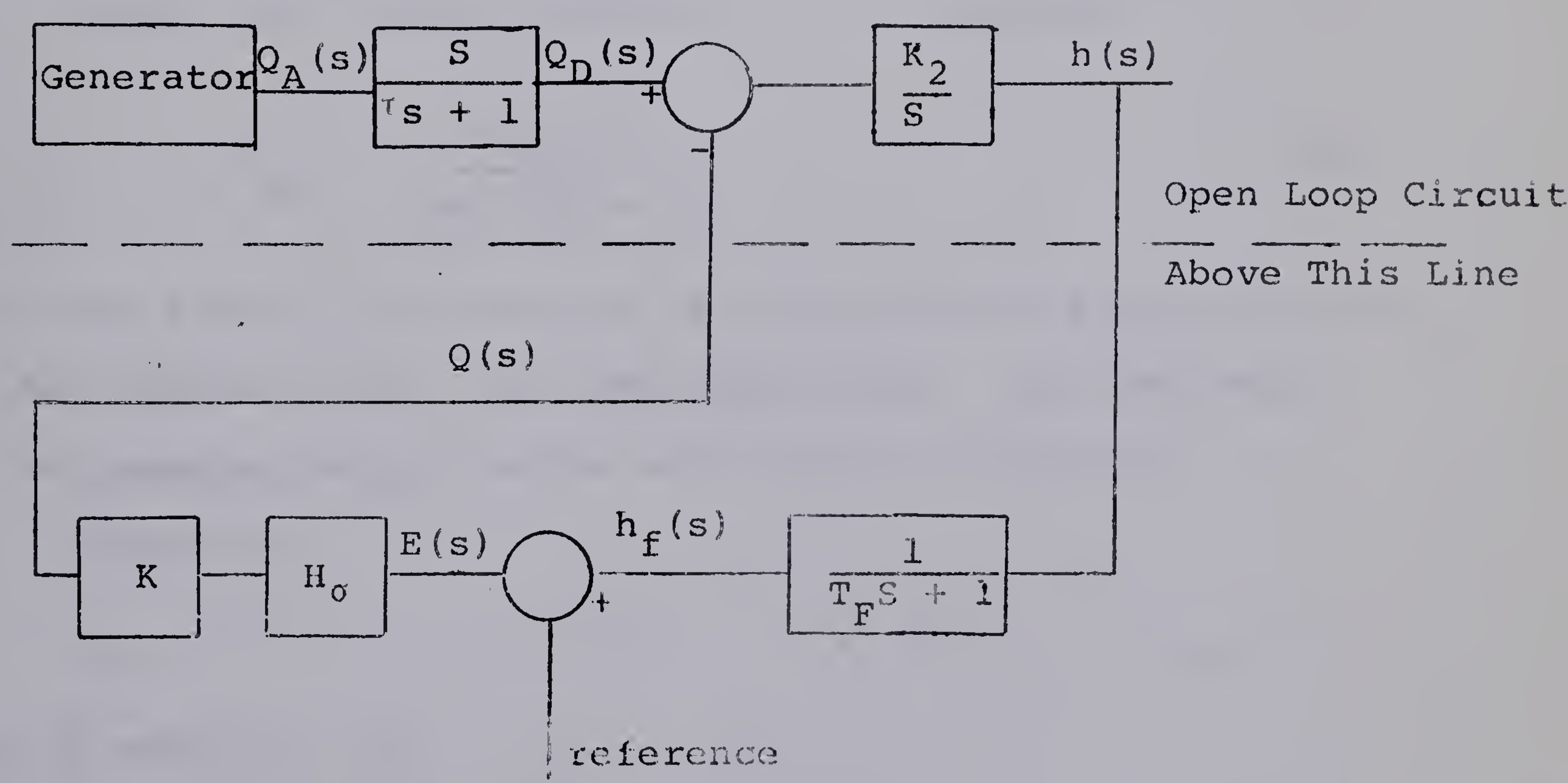

Figure 11

On the computer the control loop was broken along the dashed line in Figure 11. The Gaussian random generator was then adjusted until the rms of h above the dashed line was one. (The Gaussian random generator was then left at this setting for all random studies.) With the open loop h_{rms} equal to one, "n" is calculated as follows:

For the open loop:

$$h(S) = \left(\frac{nw_o}{S + w_o}\right)\left(\frac{S}{\tau S + 1}\right)\left(\frac{K_2}{S}\right) = \frac{K_2 nw_o}{\tau S^2 + (\tau w_o + 1)S + w_o} \tag{18}$$

By equations (10) and (11)

$$h_{ms} = \frac{1}{2\pi j}\int_{-\infty}^{\infty} \frac{(K_2 nw_o)^2 \, j \, dw}{\{\tau(jw)^2 + (\ w_o + 1)jw + w_o\}\{\tau(-jw)^2 + (\tau w_o + 1)(-jw) + w_o\}} \tag{19}$$

Using the integral tables (5-1) of reference (9)

$$h_{ms} = \frac{(K_2 nw_o)^2}{2w_o(\tau w_o + 1)} \tag{20}$$

Since the results are going to be compared with those obtained on the computer model, the constants K_2 and τ are made equal to the computer values in the analytical calculations.

Therefore,

$K_2 = 0.2 \qquad \tau = 10 \qquad w_o = 1 \qquad h_{rms} = 1$

Thus by equation (20)

$$h_{ms} = \frac{(0.2n)^2}{2(10 + 1)} = 1$$

Therefore, $\quad n = 23.4$

The Laplace transform of the Gaussian random generator output is thus $\frac{23.4}{S+1}$. (In the calculations that follow, all expressions will be derived before values are substituted. Therefore, the Gaussian random generator output will be represented by $Q_R(S) = \frac{nw_o}{S + w_o}$ until values are again substituted.)

Now with $Q_R(S)$ as the Gaussian random generator output, the transfer function is obtained for each variable in the closed control loop of Figure 11. All average values in the mathematical model are taken as zero. Therefore, the reference value in Figure 11 is zero.

Therefore, $E(S) = h_f(S)$

From the block diagram of Figure 11

$$h_f(S) = \frac{K_2}{S(T_F S + 1)} \left\{ \frac{Q_R(S) S}{\tau S + 1} - Q(S) \right\} \qquad (22)$$

Also, $Q(S) = H_\sigma K E(S)$ (23)

Now substituting equation (21) and (23) in (22)

$$E(S) = \frac{Q_R(S)\ K_2}{(\tau S + 1)(T_F S + 1)} - \frac{K\ K_2 H_\sigma\ E(S)}{(T_F S + 1)\ S} \qquad (24)$$

Rearranging equation (24)

$$E(S) = \frac{K_2 S\ Q_R(S)}{(\tau S + 1)(T_F S^2 + S + K_1 K_2 H_\sigma)} \qquad (25)$$

Letting $Q_R(S) = \frac{nw_o}{S + w_o}$ and multiplying

$$E(S) = \frac{K_2 n w_o S}{B_o S^4 + B_1 S^3 + B_2 S^2 + B_3 S + B_4} \tag{26}$$

where

$$B_o = T_F \tau$$

$$B_1 = (\tau + T_F) + w_o \tau\, T_F$$

$$B_2 = 1 + \tau K K_2 H_\sigma + w_o (T_F + \tau)$$

$$B_3 = K K_2 H_\sigma + (1 + \tau K\, K_2 H_\sigma) w_o$$

$$B_4 = w_o K K_2 H_\delta$$

By equation (23)

$$Q(S) = \frac{K K_2 H_\sigma n w_o S}{B_o S^4 + B_1 S^3 + B_2 S^2 + B_3 S + B_4} \tag{27}$$

Also, from the block diagram

$$h_f(S) = \frac{h(S)}{T_F S + 1} \tag{28}$$

Therefore, by equation (21) and (26)

$$h(S) = \frac{K_2 n w_o (T_F S + 1) S}{B_o S^4 + B_1 S^3 + B_2 S^2 + B_3 S + B_4} \tag{29}$$

Let E_{ms}, Q_{ms}, and h_{ms} equal the mean-square of the error, manipulated variable, and controlled variable respectively. Then apply equation (10) to equation (26), (27), and (29) to obtain the above three variables as functions of H_σ, the statistical describing function.

Solving equation (26) for E_{ms} and thus E_{rms}

$$E_{ms} = \frac{1}{2\pi} \int_{-\infty}^{\infty} \{(K_2 n w_o)^2 (jw)(-jw)\ dw\} / \{ [B_o(jw)^4 + B_1(jw)^3$$

$$+ B_2(jw)^2 + B_3(jw) + B_4] [B_o(-jw)^4 + B_1(-jw)^3$$

$$+ B_2(-jw)^2 + B_3(-jw) + B_4] \} \tag{29}$$

From table (5-1) of reference (9)

$$E_{ms} = \frac{(K_2 n w_o)^2 B_1}{2(B_1 B_2 B_3 - B_o B_3{}^2 - B_1{}^2 B_4)} \tag{30}$$

Now substituting in the numerical values of:

$w_o = 1$, $n = 23.4$, $K = 4$, $K_2 = 0.2$, $\tau = 10$, $T_F = 0.5$

$$E_{ms} = \frac{1}{1.019 + 8.3H_\sigma + 4.38H_\sigma{}^2} \tag{31}$$

Therefore,

$$E_{rms} = \sqrt{\frac{1}{1.019 + 8.3H_\sigma + 4.38H_\sigma{}^2}} \tag{32}$$

Keeping all other values the same but changing K to 1.9

$$E_{ms} = \frac{1}{1.019 + 3.94H_\sigma + 0.932H_\sigma{}^2} \tag{33}$$

Therefore,

$$E_{rms} = \sqrt{\frac{1}{1.019 + 3.94H_\sigma + 0.932H_\sigma{}^2}} \tag{34}$$

Now solving equation (27) for Q_{ms} and Q_{rms}

$$Q_{ms} = \frac{1}{2\pi} \int_{-\infty}^{\infty} \{(KK_2H_\sigma nw_o)^2 (jw)(-jw)dw\} / \{[B_o(jw)^4 + B_1(jw)^3$$

$$+ B_2(jw)^2 + B_3(jw) + B_4] [B_o(-jw)^4 + B_1(-jw)^3$$

$$+ B_2(-jw)^2 + B_3(-jw) + B_4] \} \qquad (35)$$

From the integral table (5-1) of reference (9)

$$Q_{ms} = \frac{(KK_2H\ nw_o)^2\ B_1}{2(B_1B_2B_3 - B_oB_3^2 - B_1^2B_4)} \qquad (36)$$

Again substituting the above numerical values with K = 4

$$Q_{ms} = \frac{H_\sigma^2}{0.0635 + 0.519H + 0.274H^2} \qquad (37)$$

Therefore,

$$Q_{rms} = \frac{H\sigma}{\sqrt{0.0635 + 0.519H + 0.274H_\sigma^2}} \qquad (38)$$

For the above values with K = 1.9

$$Q_{ms} = \frac{H_\sigma^2}{0.2835 + 1.095H + 0.2595H_\sigma^2} \qquad (39)$$

Therefore,

$$Q_{rms} = \frac{H_\sigma}{\sqrt{0.2835 + 1.095H + 0.2595H_\sigma^2}} \qquad (40)$$

Now solving equation (29) for h_{ms} and h_{rms}

$$h_{ms} = \frac{1}{2\pi} \int_{-\infty}^{\infty} \{(K_2 n w_o)^2 (T_F (jw)^4 - (jw)^2)\, dw\} / \{[B_o(jw)^4 + B_1(jw)^3$$

$$+ B_2(jw)^2 + B_3(jw) + B_4]\, [B_o(-jw)^4 + B_1(-jw)^3$$

$$+ B_2(-jw)^2 + B_3(-jw) + B_4]\} \tag{41}$$

From the integral table (5-1) of reference (9)

$$h_{ms} = \frac{(K_2 n w_o)^2 (T_F B_3 + B_1)}{2(B_1 B_2 B_3 - B_o B_3^2 - B_1^2 B_4)} \tag{42}$$

Again substituting the above numerical values with K = 4

$$h_{ms} = \frac{15.75 + 2.2H_\sigma}{15.8 + 128.9H_\sigma + 68.0H_\sigma^2} \tag{43}$$

Therefore,

$$h_{rms} = \sqrt{\frac{15.75 + 2.2H_\sigma}{15.8 + 128.9H_\sigma + 68.0H_\sigma^2}} \tag{44}$$

The above values with K = 1.9

$$h_{ms} = \frac{15.75 + 1.046H_\sigma}{15.8 + 61.1H_\sigma + 14.49H_\sigma^2} \tag{45}$$

Therefore,

$$h_{rms} = \sqrt{\frac{15.75 + 1.046H_\sigma}{15.8 + 61.1H_\sigma + 14.49H_\sigma^2}} \tag{46}$$

Thus, E_{rms}, Q_{rms} and h_{rms} are all given as functions of H_σ, the statistical describing function. The statistical describing function must now be determined in terms of the input rms for the various nonlinearities. It can be seen from Figure 11 that this input rms value to the nonlinearity is E_{rms}. For simplicity, assume E_{rms} to be a biased estimate of σ. Now since the average value of e is zero, the rms and standard deviation are equal. Therefore, it remains to calculate $\overline{f(v)}$ and to apply equation (17) for each nonlinearity to obtain the statistical describing functions.

The various nonlinearities for which H_σ, the statistical describing function, will be obtained are $e|e|$, e^3, $|e|e^3$, and $\left|\frac{e^{3/2}}{e}\right|$. The different H_σ's will then be studied for their effect on the control loop of Figure 11.

Calculation of H_σ for $e|e|$

Let $(e|e|)^2 = v^4$ to comply with the above symbols in the theoretical discussion.

Applying equation (16)

$$\overline{f(v)} = \int_{-\infty}^{\infty} \frac{v^4 \; e^{-v^2/2\sigma^2}}{\sigma\sqrt{2\pi}} \, dv$$

$$= 3\sigma^4$$

Applying equation (17)

$$H_\sigma = \sqrt{\frac{3\sigma^4}{\sigma^2}} = \sigma\sqrt{3}$$

Therefore,

$$H_\sigma = E_{rms} \sqrt{3} \tag{47}$$

Calculation of H_σ for e^3

Again let $(e^3)^2 = v^6$

Applying equation (16)

$$\overline{f(v)} = \int_{-\infty}^{\infty} \frac{v^6 e^{-v^2/2\sigma^2}}{\sigma \sqrt{2\pi}} dv$$

$$= \frac{15\sigma^6}{2}$$

Applying equation (17)

$$H_\sigma = \sqrt{\frac{\frac{15}{2}\sigma^6}{\sigma^2}} = 2.74\sigma^2$$

Therefore,

$$H_\sigma = 2.74 \, (E_{rms})^2 \tag{48}$$

Calculation of H_σ for $|e|e^3$

Again let $(|e|e^3)^2 = v^8$

Applying equation (16)

$$\overline{f(v)} = \int_{-\infty}^{\infty} \frac{v^8 e^{-v^2/2\sigma^2}}{\sigma \sqrt{2\pi}} dv$$

$$= 52.5\sigma^8$$

Applying equation (17)

$$H_\sigma = 7.2\sigma^3$$

Therefore,

$$H_\sigma = 7.2 \, (E_{rms})^3 \tag{49}$$

Calculation of H_σ for $\frac{|e^{3/2}|}{e}$

Again let $\left(\frac{|e^{3/2}|}{e}\right)^2 = |v|$

Applying equation (16)

$$\overline{f(v)} = \int_{-\infty}^{\infty} \frac{|v|\ e^{-v^2/2\sigma^2}}{\sigma\sqrt{2\pi}}\ dv$$

$$= \frac{\sigma}{\sqrt{2\pi}}$$

Applying equation (17)

$$H_\sigma = \frac{0.639}{\sqrt{\sigma}}$$

Therefore,

$$H_\sigma = \frac{0.639}{\sqrt{E_{rms}}} \tag{50}$$

The solutions of equations (47) to (50) with equations (32) and (34) were carried out graphically. Also, the equations(38) and (40) were plotted so that the effects of the different solutions could be seen on the manipulated variable, Q_{rms}. Since h_{rms} and E_{rms} curves follow one another closely, only the E_{rms} curve was plotted. (The important points on the h_{rms} curve are marked by a cross (+).) This extension, of including the manipulated variable curve along with values of h_{rms} and the two curves of E_{rms} vs. H_σ

needed for solution, is important. The reason is that by plotting the curves of different nonlinearities, one can predict the effect the nonlinearity will have on both Q_{rms} and h_{rms}. This gives the designer the power to choose those nonlinearities which will be suitable from an rms standpoint. Further elimination can then be carried out using other criteria, such as, lowest ITAM.

Each nonlinearity for which a statistical describing function was developed above will now be discussed in terms of its effect on h_{rms}, the controlled variable, and Q_{rms}, the manipulated variable. First, note Figure 15 on which equation (32) and (44) are plotted. Figure 15 illustrates how closely the h_{rms} and E_{rms} curves follow one another. Also, on Figures 12A, 12B, 13 and 14, the points (b) and (d) are linear values of E_{rms} and Q_{rms}, respectively and the points (a) and (c) are the values of E_{rms} and Q_{rms} respectively produced by the nonlinearity under discussion. Also, all graphs are for a gain of four unless otherwise stated.

The nonlinearity $\frac{|e^{3/2}|}{e}$, which is described by equation (50), has a solution at point (a) on Figure 14. Point (c) on Figure 14 is the corresponding Q_{rms} value that would result if the nonlinearity were used in the control loop. Thus, as compared to the linear system, this nonlinearity, $\frac{|e^{3/2}|}{e}$, brings about a small decrease in E_{rms} and h_{rms}

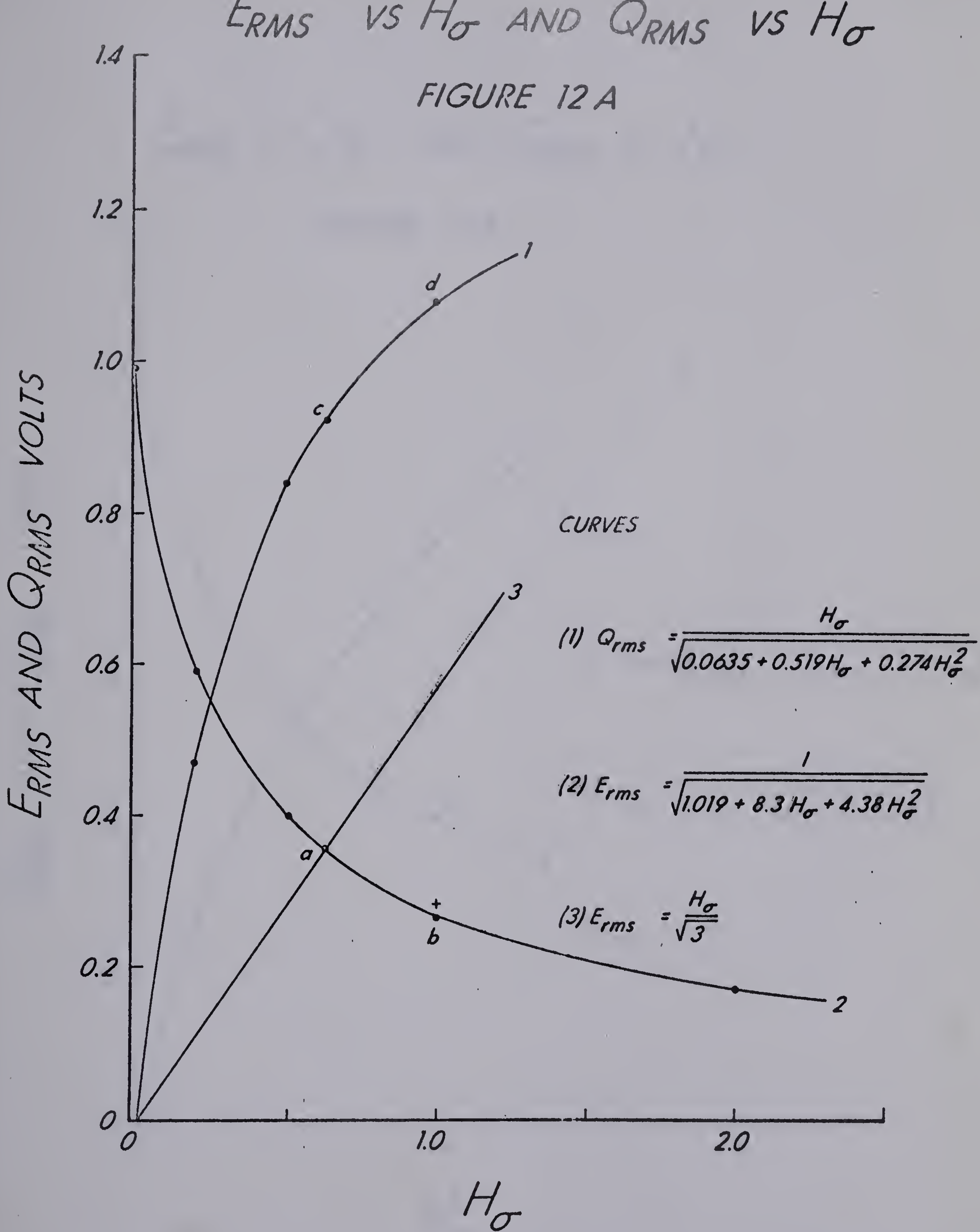
ERMS VS Hσ AND QRMS VS Hσ
FIGURE 12 A
ERMS AND QRMS VOLTS
1.4
1.2
1.0
0.8
0.6
0.4
0.2
0
0
1.0
2.0
Hσ
a
b
c
d
1
2
3
CURVES
(1) $Q_{rms} = \frac{H_\sigma}{\sqrt{0.0635 + 0.519 H_\sigma + 0.274 H_\sigma^2}}$
(2) $E_{rms} = \frac{1}{\sqrt{1.019 + 8.3 H_\sigma + 4.38 H_\sigma^2}}$
(3) $E_{rms} = \frac{H_\sigma}{\sqrt{3}}$

E_{RMS} VS H_σ AND Q_{RMS} VS H_σ

FIGURE 12 B

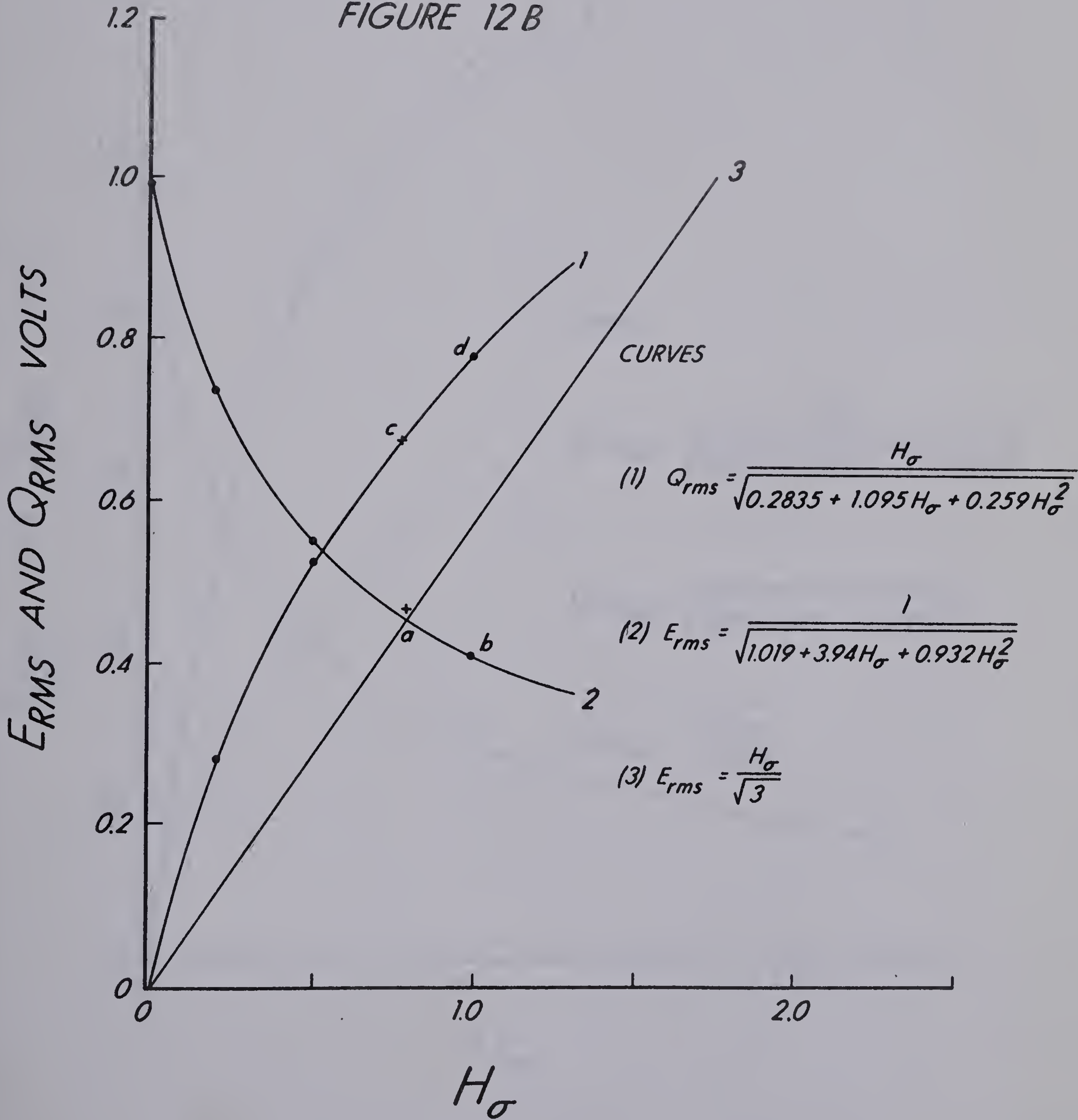

E_{RMS} VS H_σ AND Q_{RMS} VS H_σ

FIGURE 13

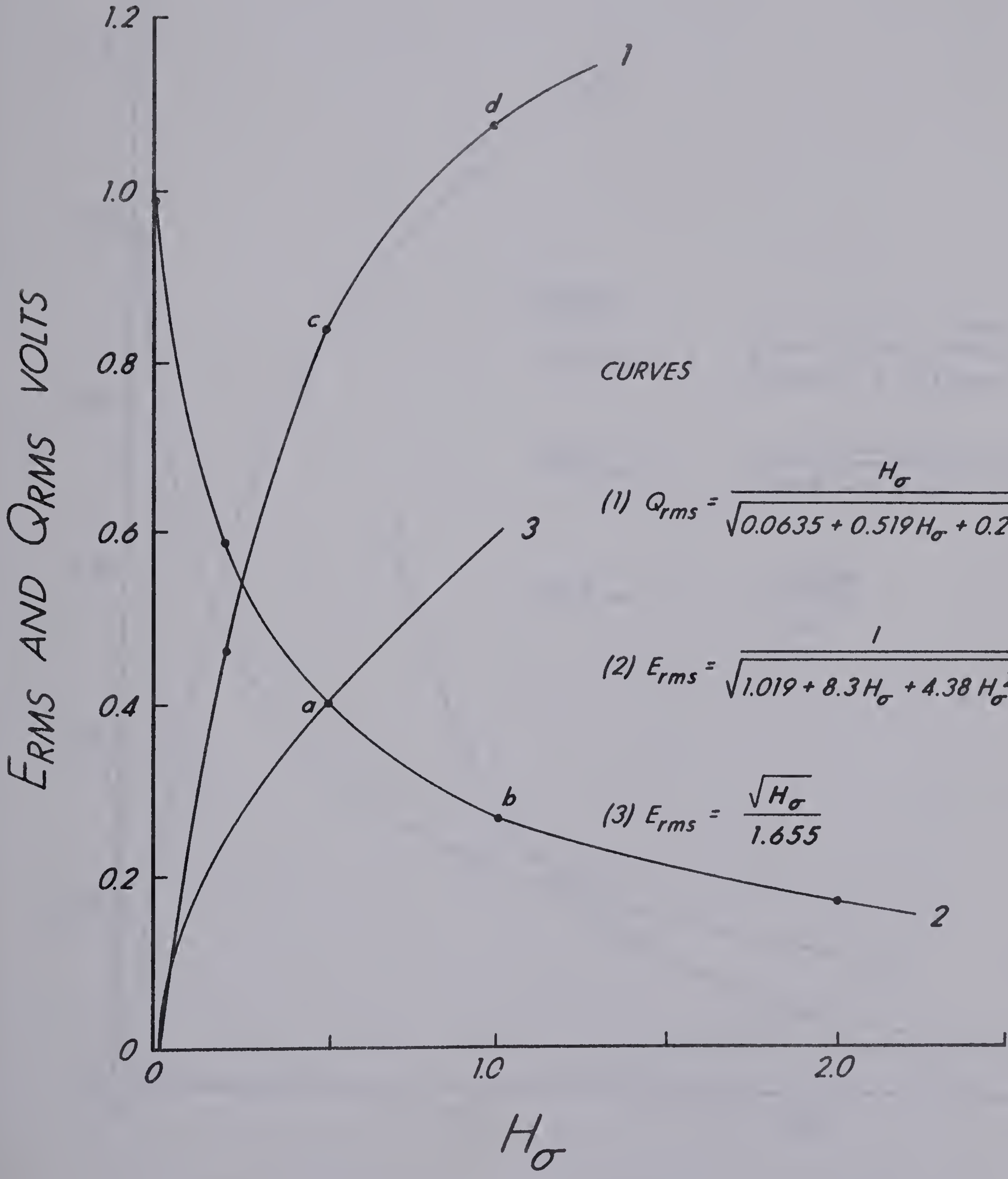

E_{RMS} VS $H\sigma$ AND Q_{RMS} VS $H\sigma$

FIGURE 14

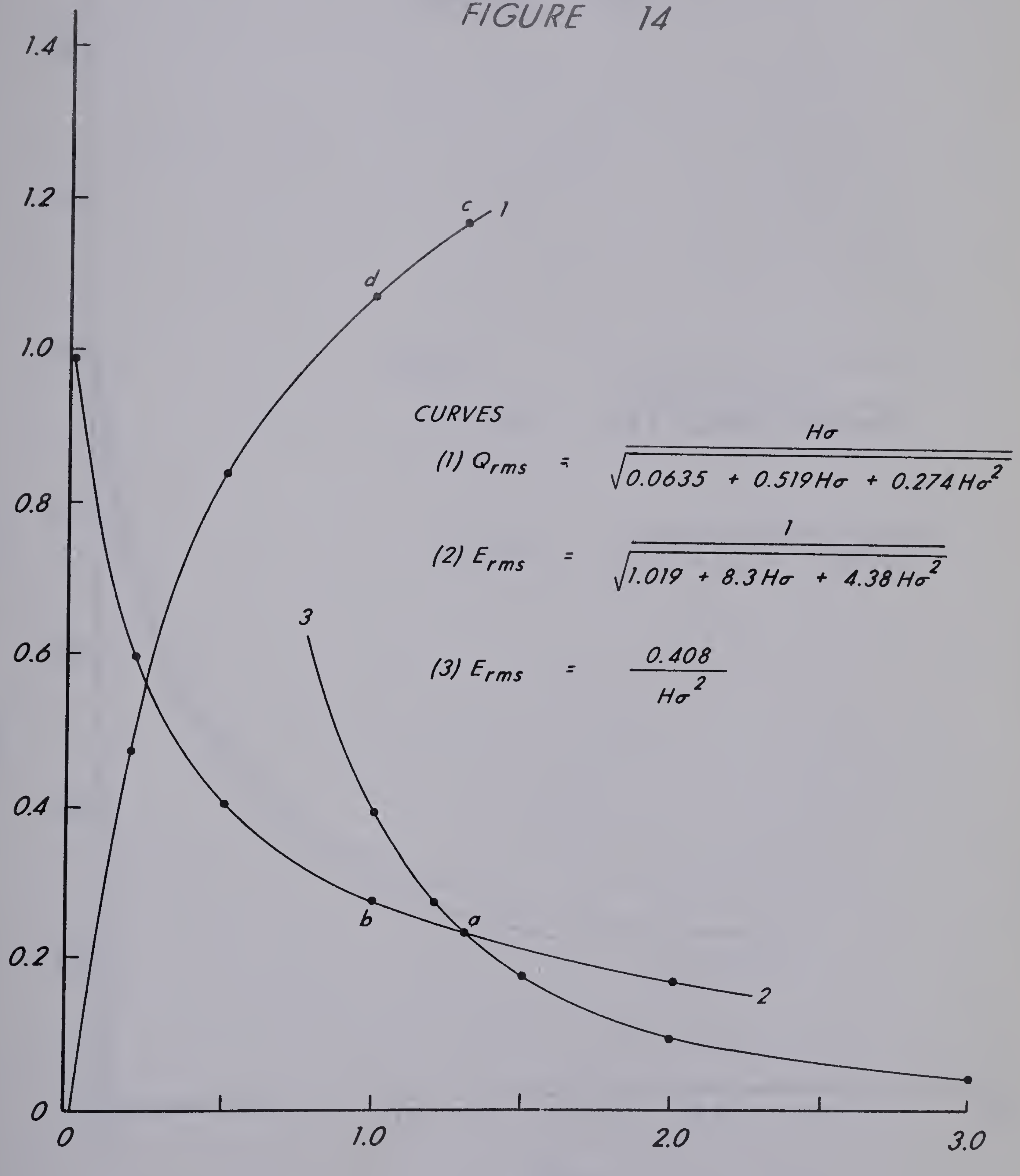

COMPARISON OF E_{RMS} AND h_{RMS}

FIGURE 15

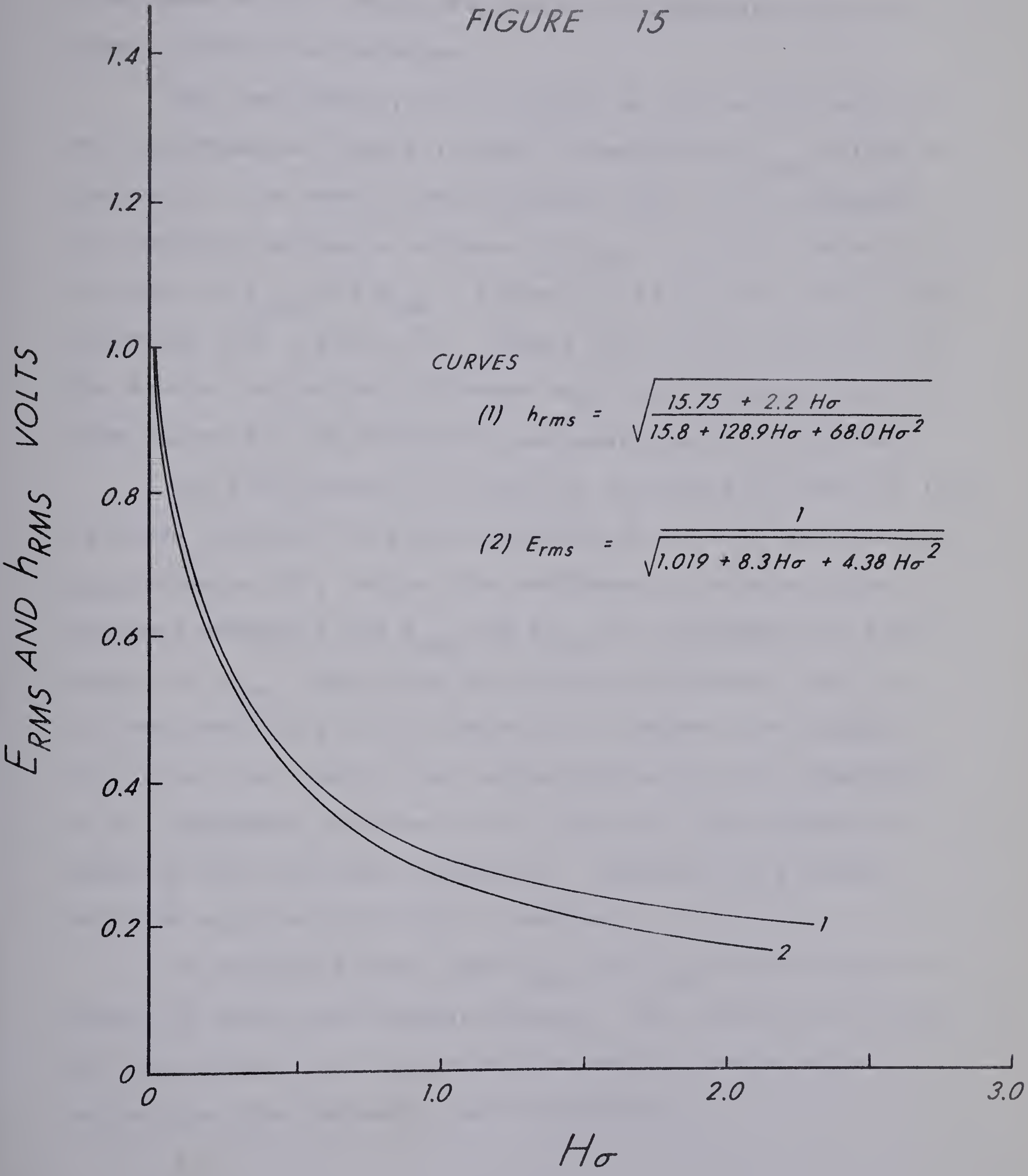

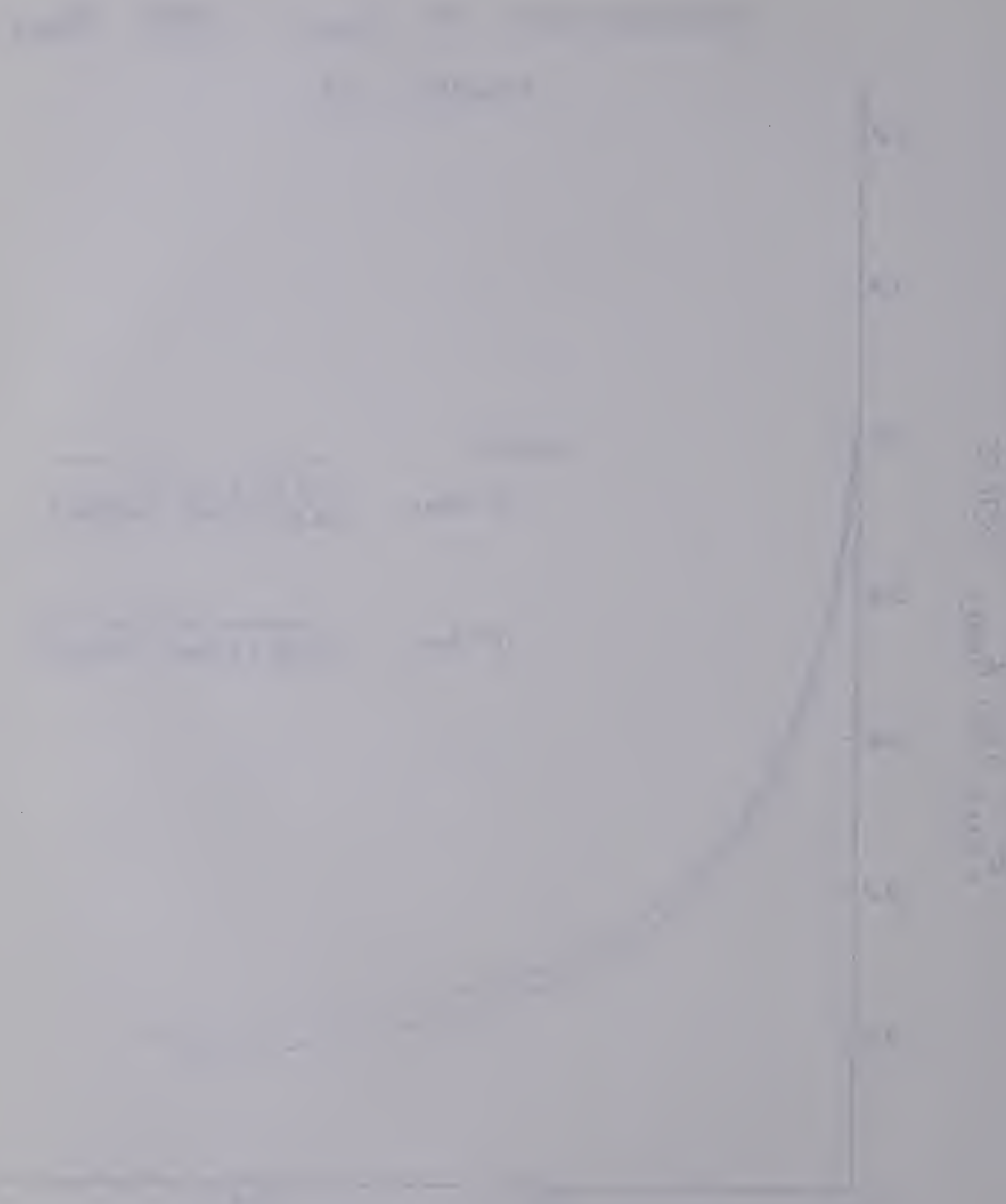

and a small increase in Q_{rms}. This is unacceptable from the standpoint of this study and thus this nonlinearity was not given further consideration.

The nonlinearity $e|e|$ is shown in Figures 12A and 12B with solutions at points (a) and corresponding Q_{rms} values at points (c). As seen on both Figures, this is an acceptable nonlinearity because a decrease in Q_{rms} is brought about by an increase in E_{rms} and h_{rms}. Figure 12A is for the control loop operating with a gain of 4. Figure 12B is for a gain of 1.9. The reason for the two different gains will be seen when the ITAM values for the different nonlinearities are discussed.

The nonlinearity e^3, which is described by equation (48), is shown on Figure 13 with a solution at (a) and corresponding Q_{rms} value at (c). Again this nonlinearity is acceptable from rms viewpoint for E_{rms} and h_{rms} are increased for a decrease in Q_{rms}. Note that this change is greater than for the nonlinearity $e|e|$ on Figure 12A. However, the author will show later that e^3 and higher powers are not acceptable, in his judgement, because of the resulting ITAM values produced by the high power functions. Therefore, the Figure with the solution for $|e|e^3$ is omitted.

As mentioned above, the h_{rms} and E_{rms} curves shown on Figure 15 follow one another closely. The difference between the two, however, is the amount the rms is lowered by removing the high frequency load disturbances.

The above-mentioned figures will be discussed again in the experimental section.

Summary

This section has done basically three things. First, a mathematical model for the system was produced. Second, the system was checked for stability under linear conditions and two cases of nonlinear conditions. Finally, a method of calculating rms values for linear and nonlinear control loops was explained. The method was then used to calculate and predict rms value changes due to given nonlinearities. However, no ITAM values were calculated. These are taken with the analogue computer in the next section.

Experimental Report

The following experimental report is divided into two sections. The first section is concerned with the mathematical model programmed for the analogue computer. With the computer model, the analytical rms calculations are checked and ITAM values are gathered for the different types of control. The second section deals with work done to verify the mathematical model used in this study. Actual field equipment was set up and operated for this part of the study. The two reports that follow are written as individual laboratory studies.

A. Computer Studies

Purpose - The computer studies were carried out to check the mathematical calculations in the theory section and to calculate ITAM values for different gain and step sizes. From the data gathered, it would then be possible to conclude which nonlinear function, if any, was the best for the system of Figure (4).

Apparatus - The equipment used was a 75 amplifier Pace analogue computer and an 8 channel Pace recorder and a Gaussian random signal generator (type RG77) manufactured by Servomex Controls Limited. (The frequency band of the generator is shown on Figure 16A.)

Procedure - The procedure for the work done on the computer was divided into three operations: one, to set the program up generally; two, to set up and operate the program

BODE' AMPLITUDE PLOTS SHOWING FREQUENCY BAND WIDTHS

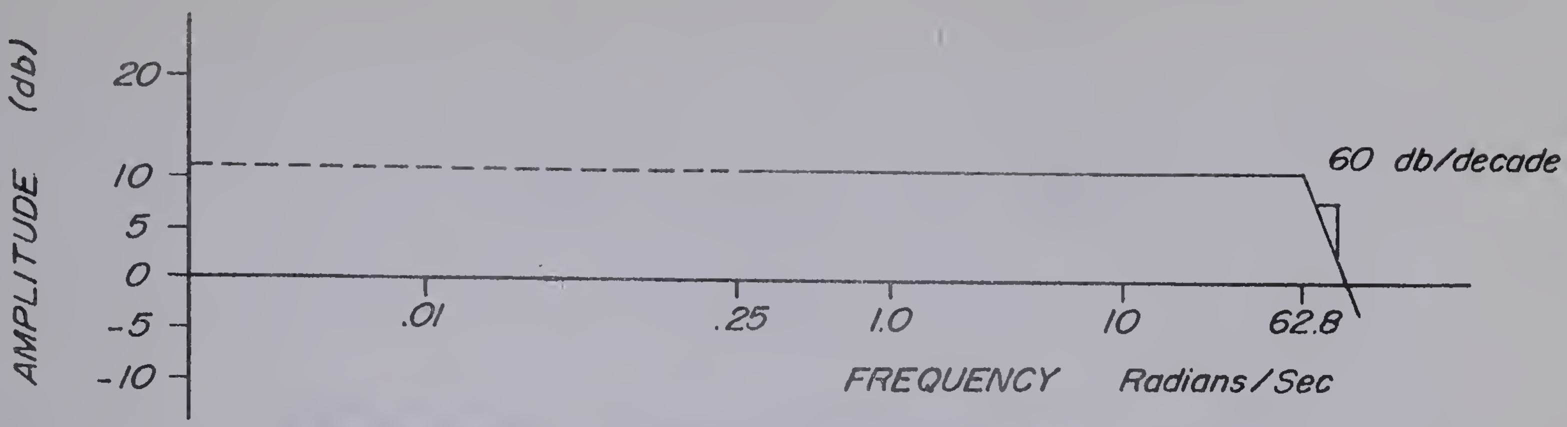

RANDOM GENERATOR FREQUENCY BAND

FIGURE 16A

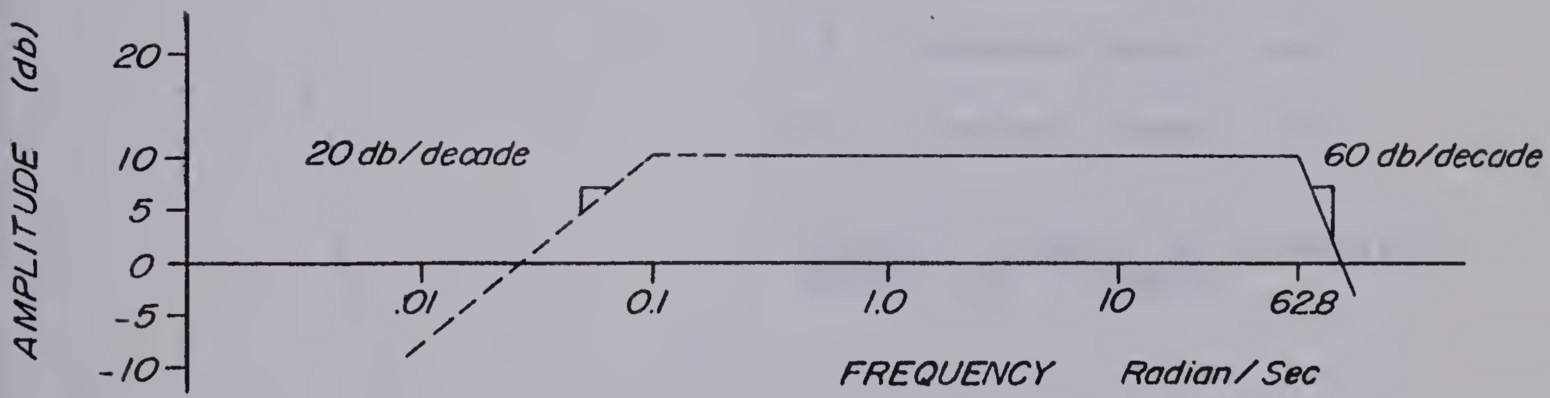

FREQUENCY BAND INPUT TO COMPUTER MODEL

FIGURE 16B

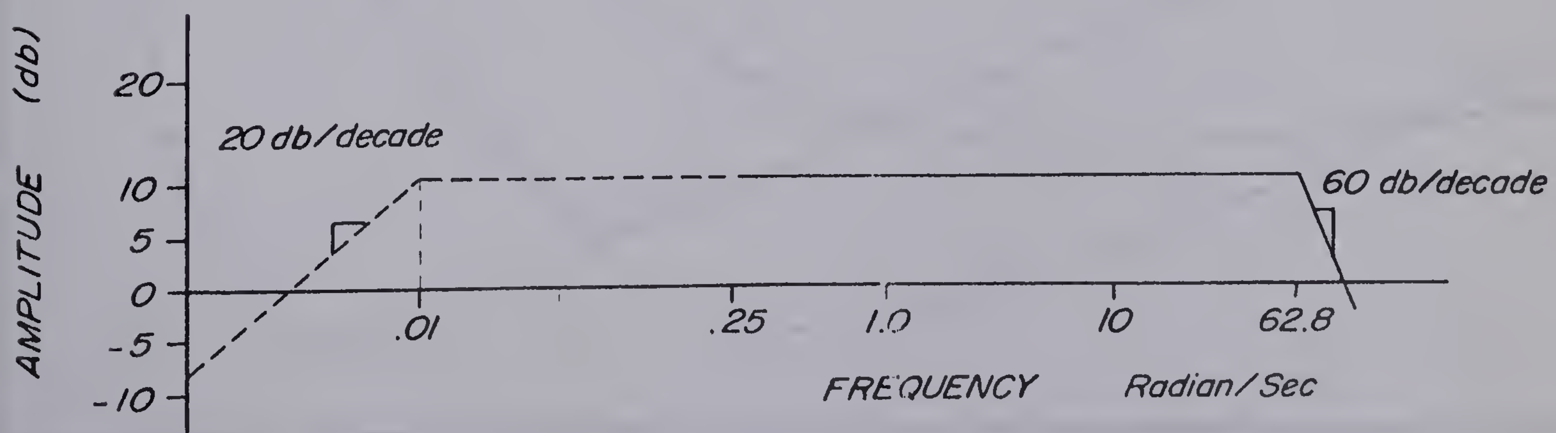

FREQUENCY BAND INPUT TO FIELD EQUIPMENT

FIGURE 16C

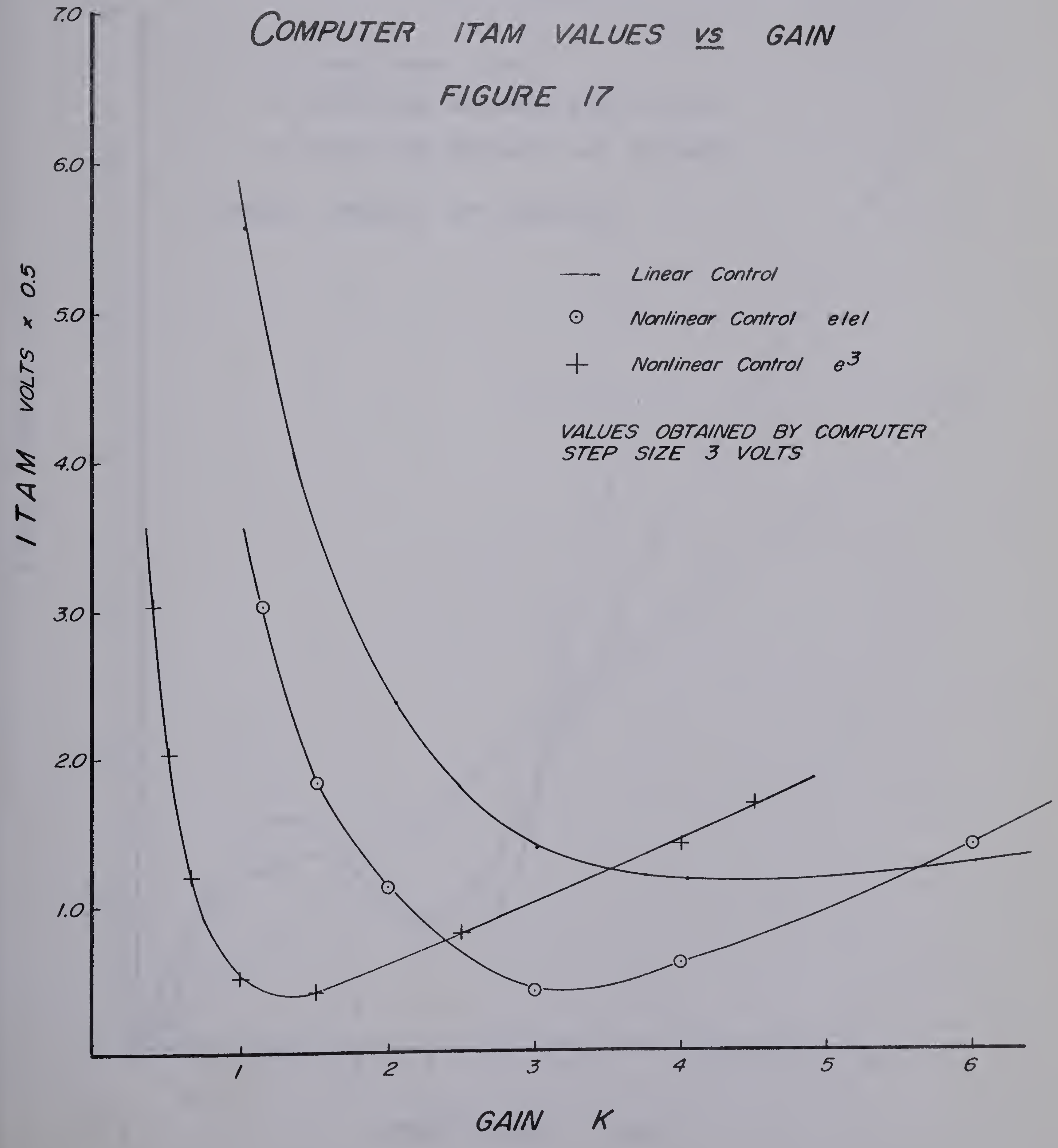
COMPUTER ITAM VALUES vs GAIN
FIGURE 17
Linear Control
Nonlinear Control e/e/
Nonlinear Control e3
VALUES OBTAINED BY COMPUTER
STEP SIZE 3 VOLTS
ITAM VOLTS x 0.5
7.0
6.0
5.0
4.0
3.0
2.0
1.0
1
2
3
4
5
6
GAIN K

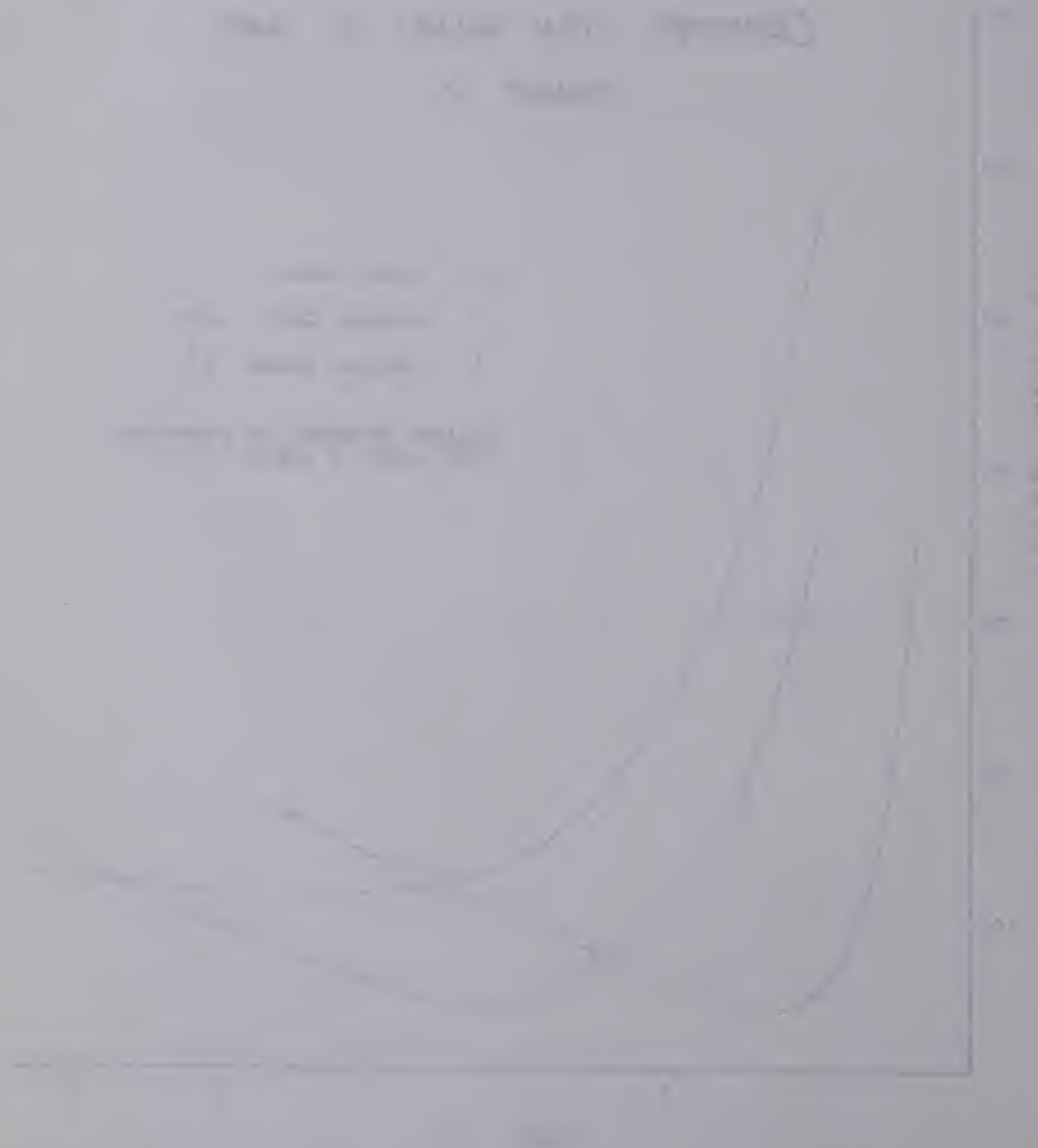

ITAM VALUES vs STEP SIZE

FIGURE 18

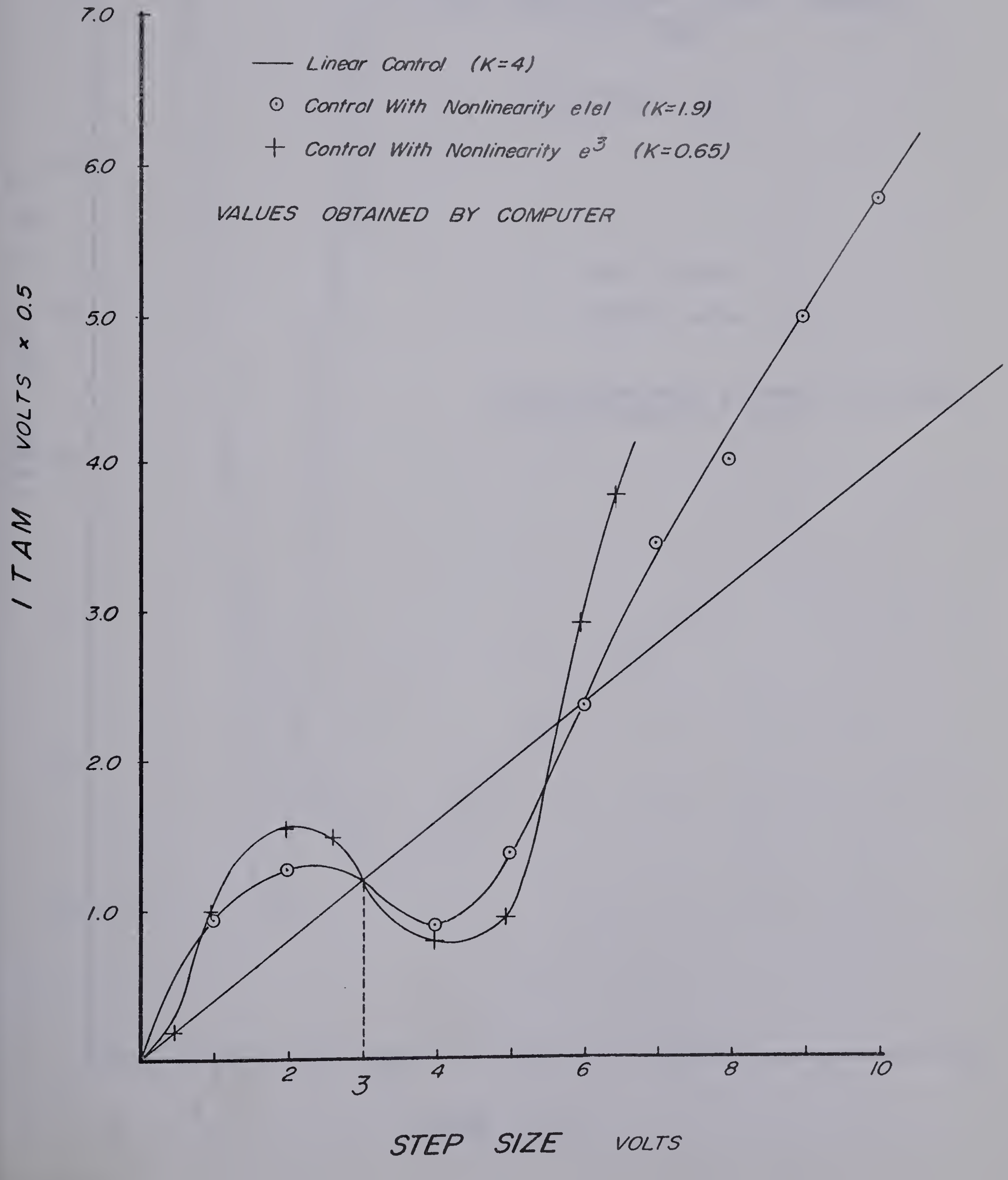

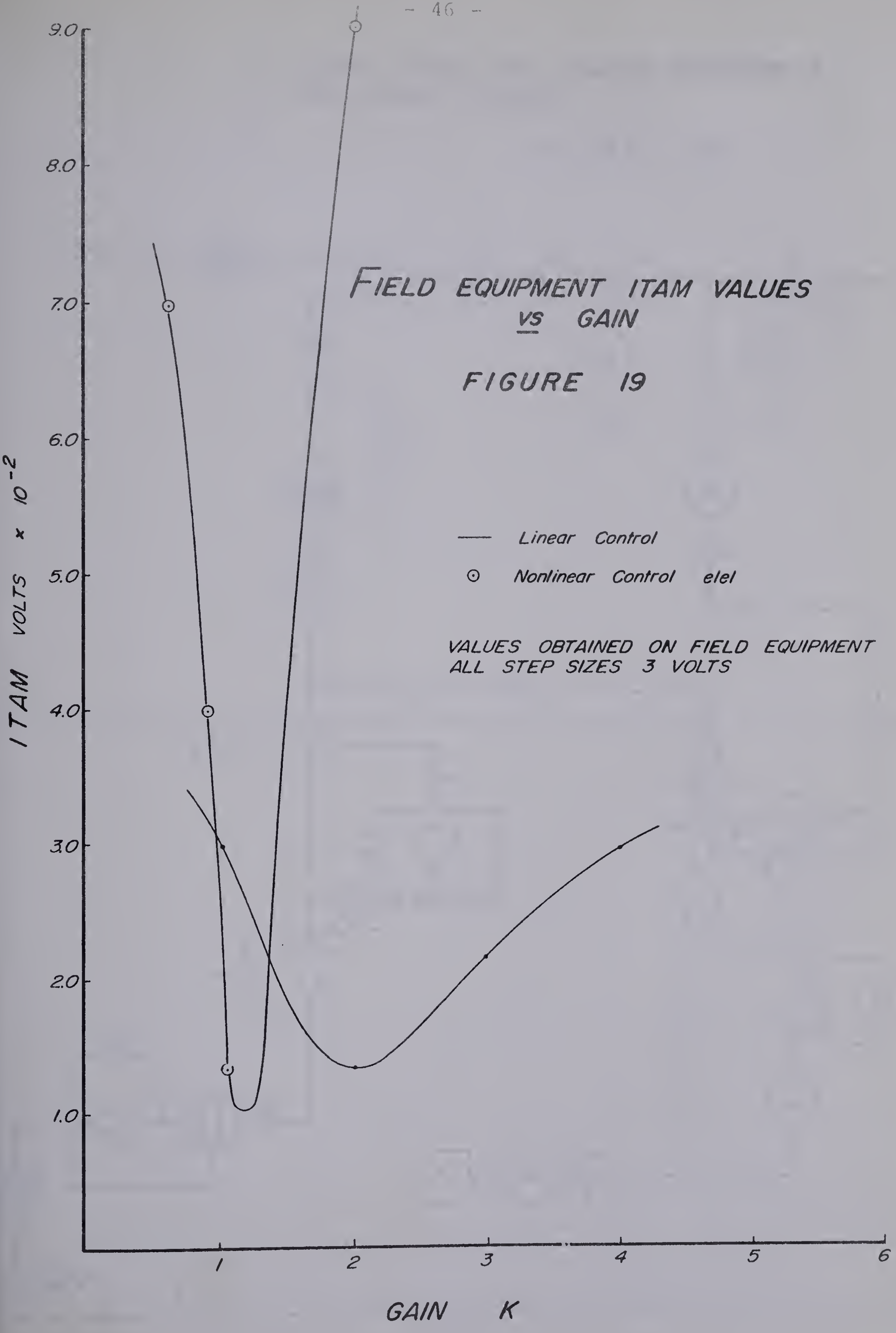
FIELD EQUIPMENT ITAM VALUES
VS GAIN
FIGURE 19
Linear Control
Nonlinear Control elel
VALUES OBTAINED ON FIELD EQUIPMENT
ALL STEP SIZES 3 VOLTS
ITAM VOLTS × 10^{-2}
9.0
8.0
7.0
6.0
5.0
4.0
3.0
2.0
1.0
1
2
3
4
5
6
GAIN K

LINEAR SYSTEM WITH RANDOM GENERATOR & MEAN SQUARE CIRCUITS

FIGURE 20

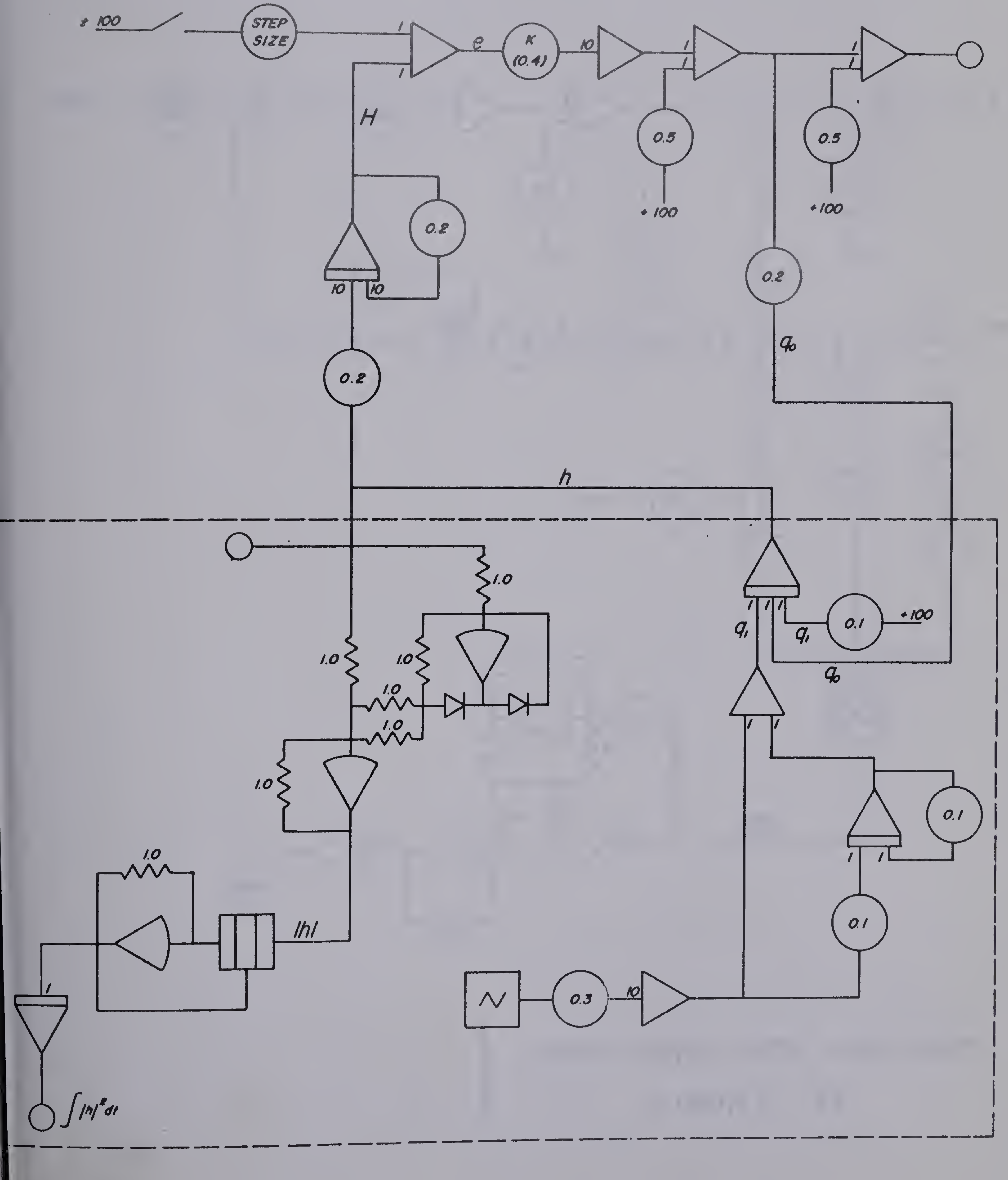

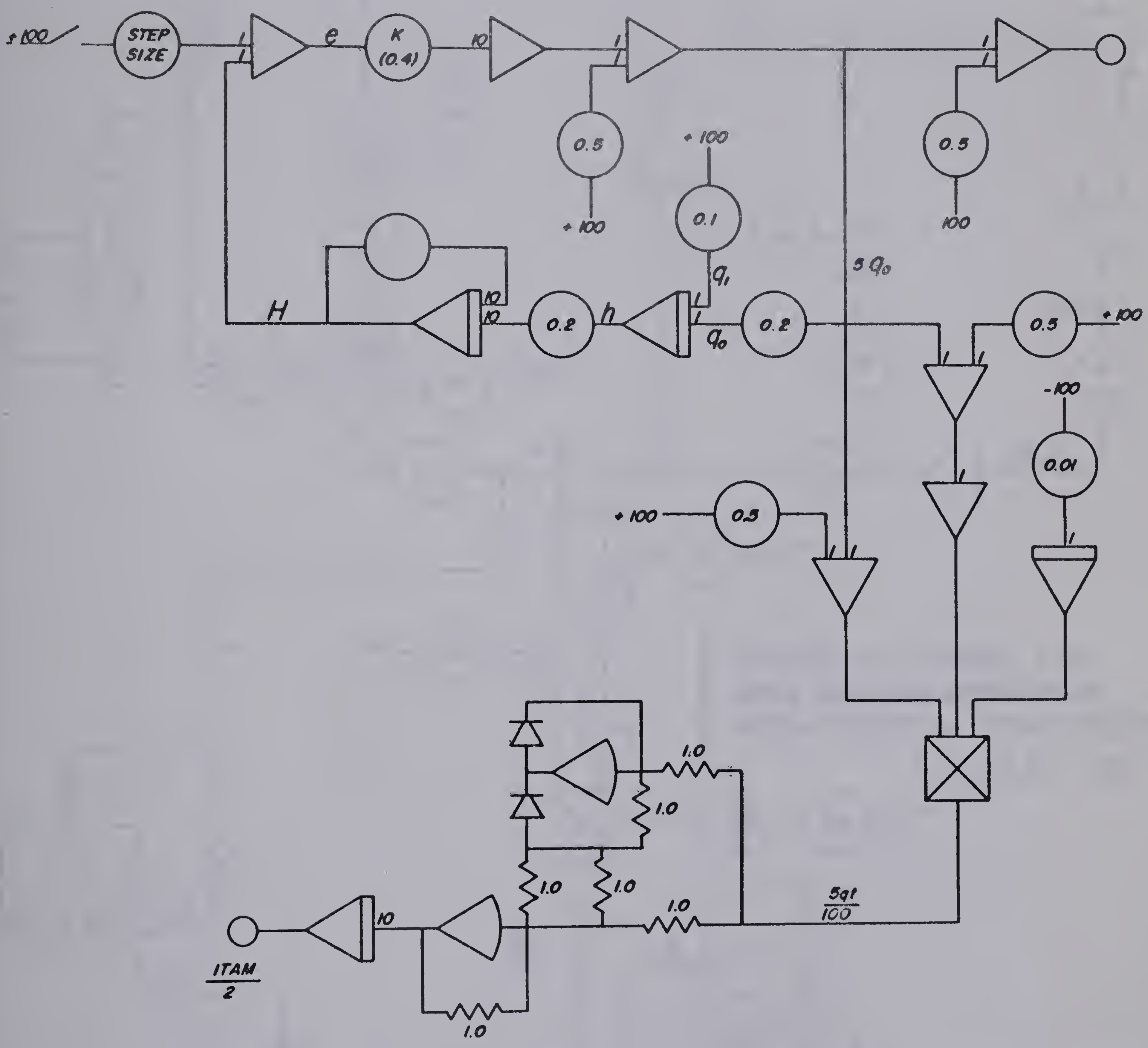

LINEAR SYSTEM WITH ITAM CIRCUIT

FIGURE 21

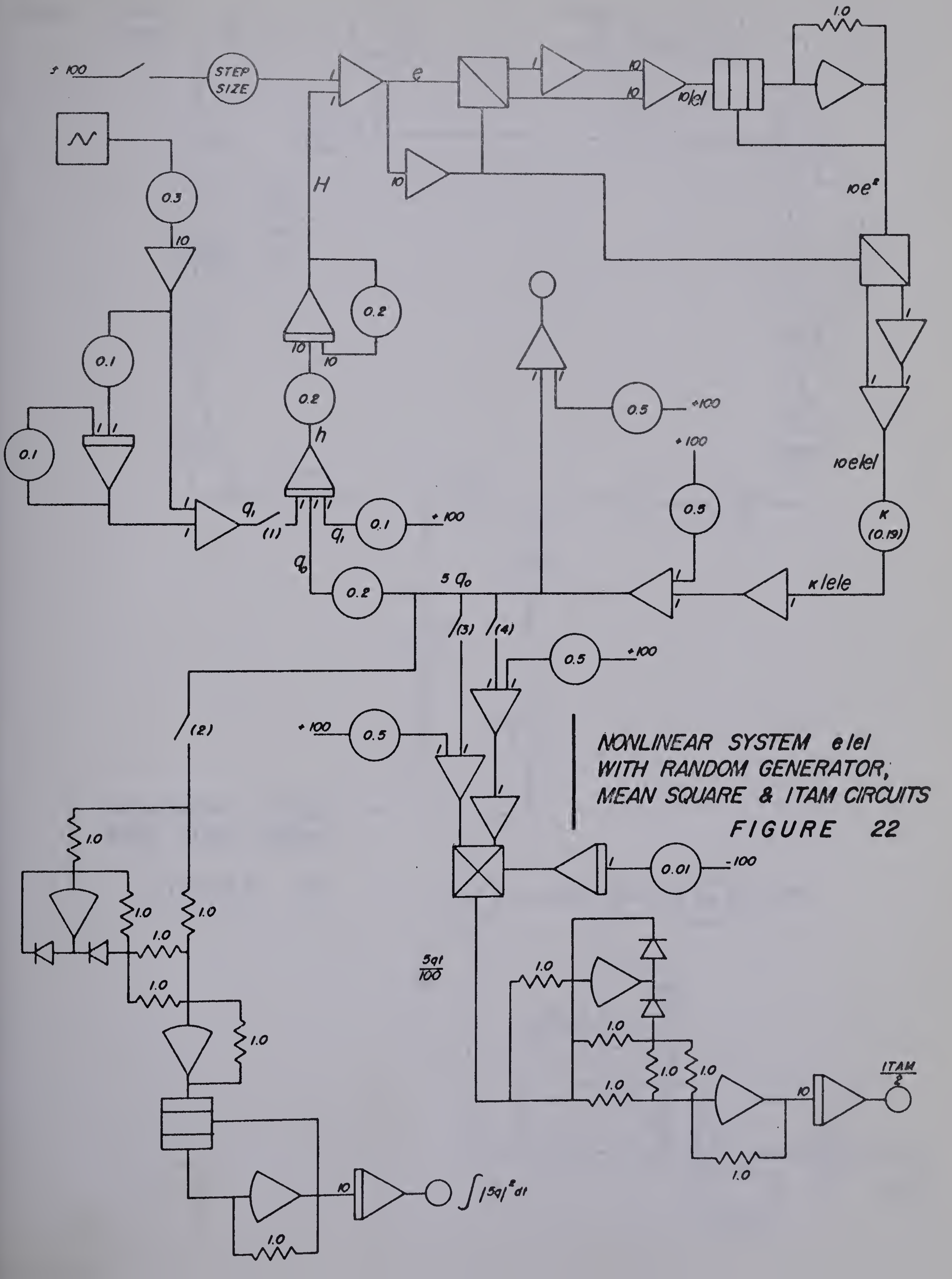

NONLINEAR SYSTEM e|e|
WITH RANDOM GENERATOR,
MEAN SQUARE & ITAM CIRCUITS

FIGURE 22

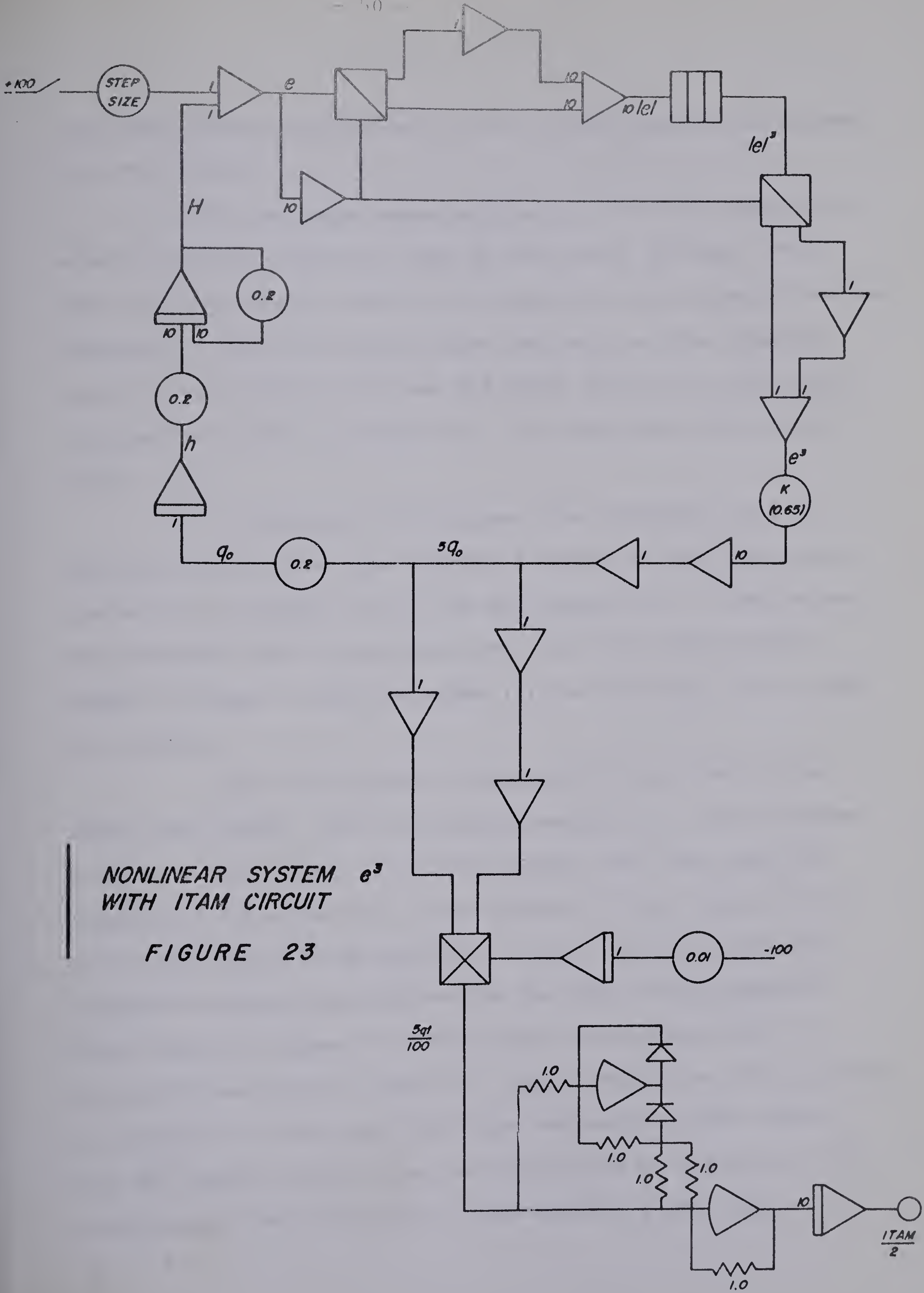

NONLINEAR SYSTEM e^3
WITH ITAM CIRCUIT

FIGURE 23

for ITAM studies; and three, to set up and operate the program for rms studies:

1) The analogue computer programs for this study were scaled to be ten times as fast as the actual process. This same time scaling had then to be applied to the Gaussian random generator. Thus, the input which was fed into the computer model is that shown in Figure 16B while that fed to the field equipment is shown in Figure 16C. No magnitude scaling was done.

2) To determine ITAM values, the computer programs were as shown on the flow charts of Figure 21 for the linear system and of Figure 23 for the nonlinearity e^3. ITAM values were obtained for the nonlinearity $e|e|$ using the program shown on Figure 22 with switches (1) and (2) open and (3) and (4) closed.

With the computer components as arranged in the above flow charts, the following procedure was used to gather ITAM data for Figures 17 and 18. First, the step size was fixed at 3 volts for the linear program. (The reason why 3 volts was used will be explained later.) The gain was then changed to obtain the information for the "linear control" curve shown on Figure 17. This was then repeated for the two nonlinearities $e|e|$ and e^3. These results are also plotted on Figure 17. The lowest and thus the optimum ITAM value for the linear control loop was then noted on Figure 17. (It occurred at a gain of four.) The smallest gains which

produced the same ITAM values as the linear optimum for the two nonlinearities $e|e|$ and e^3 were then chosen from Figure 17. The gain value of 1.9, chosen for the nonlinearity $e|e|$, was then set on the program shown on Figure 22. Similarly, the gain of 0.65, chosen for the nonlinearity e^3, was set on the program shown on Figure 23. With the gains fixed, the step sizes for both the programs shown on Figure 22 and 23 were changed to gather the data for Figure 18. This completed the ITAM studies.

3. In view of the results shown on Figures 17 and 18, the decision was made to drop the nonlinearity e^3 and to use the nonlinearity $e|e|$ with a gain of 1.9. Thus, rms values were only calculated for the linear system and the nonlinear system with $e|e|$. This was done, on the computer, using the components as arranged in the flow charts of Figure 20 and 22 respectively. For rms calculations switches (3) and (4) were open and (1) and (2) were closed on Figure 22.

For the rms calculations, the Gaussian random generator had to first be set so as to give a value of n, as mentioned in the theory section, of 23.4. This was done by using the open loop circuit that is contained within the dashed rectangle on Figure 20. Using only the above open loop circuit, the Gaussian random generator amplitude was adjusted until the rms value of h was 1. By the calculations in the theory section, n was then 23.4. With the Gaussian random generator left at this setting, the control loop of

Figure 20 was then closed and the rms values throughout the loop were measured. This same procedure was then repeated for the nonlinear system shown on Figure 22. This ended the rms investigations.

Results - The ITAM values, as mentioned above, were plotted on Figures 17 and 18. The fluctuations of the manipulated variable and controlled variable from which the rms values were calculated are shown on Figures 28 and 29, respectively. Figure 28 compares the movement of the manipulated variables for the linear system and the nonlinear system $e|e|$ under the same load disturbance. Figure 29 compares the controlled variables for the same systems under the same load disturbance. The differences between the two types of control were such that the nonlinear system had a manipulated variable rms 39% lower than the linear system and a controlled variable rms 67% higher.

Conclusions and Discussion - The ITAM results showed that the nonlinear functions $e|e|$ and e^3 were first worse than the linear controller (see Figure 18) then better and then worse again as the step change sizes were increased. The results also showed that e^3 varied more from the linear controller than $e|e|$ by a considerable amount. The nonlinearity e^3 had a shorter range of step sizes than $e|e|$ for which its ITAM values were lower and then better than the linear controller values. Thus, because of the desire to have low values of ITAM for a wide range of step sizes, $e|e|$

was chosen and e^3 and higher powers discarded. The decision to discard the higher powers was also influenced by the fact that the ITAM values increased very rapidly above 6 volts and just below 3 volts as seen on Figure 18.

The rms values of the linear and nonlinear ($e|e|$) showed that the analytical predictions were quite good. A 38% decrease in the manipulated variable was predicted (difference between (d) on Figure 12A and (c) on Figure 12B) for an increase of 64.5% in the controlled variable (difference between cross (+) on Figure 12A and cross on Figure 12B). Instead a 39% decrease was obtained in the manipulated variable for an increase of 67% in the controlled variable. The actual voltage values of the manipulated variable and controlled variable agreed within 5% of the analytical values. Both values were low on the computer. This could be due partly to the fact that the high frequency filter in the Gaussian random generator was neglected in the analytical calculations.

The computer results show that $e|e|$ is a successful nonlinear controller. If the nonlinear controller, $e|e|$, is set properly, it can give a lower ITAM value than the linear controller and still lower the rms of the manipulated variable considerably. Also, should the step size be outside the region where the nonlinear controller ITAM value is higher than that for the linear controller, the difference will not be drastic. All that remains now is to confirm the above results on the field equipment.

B. Field Equipment Studies

Purpose - The purpose of conducting the tests on the field equipment was to check the accuracy of the mathematical model and to see if the operations as described on the computer could be carried out on the field equipment.

Apparatus - The equipment used was as follows: an Applied Dynamics 32 amplifier analogue computer, two Foxboro needle valves with pneumatic motors, one Foxboro differential pressure cell for liquid level measurements, a Gaussian random signal generator (Type RG77) made by Seromex Controls Limited, and three Honeywell current to pressure and pressure to current transducers for communication between the process and the computer.

Procedure - The procedure again consisted of three steps.

1) The first step was to assemble the apparatus such that any one of the arrangements shown on Figure 24, 25, 26 and 27 could be coupled together easily. With the field equipment there was no time or magnitude scaling. Because of this, the time constant on the low frequency filter was reduced by a factor ten from the time scaled computer value (see Figure 16C). This was done to make the inputs to the computer model and the field equipment approximately the same.

LINEAR CONTROL CIRCUIT
ON FIELD EQUIPMENT
WITH ITAM CIRCUIT

FIGURE 24

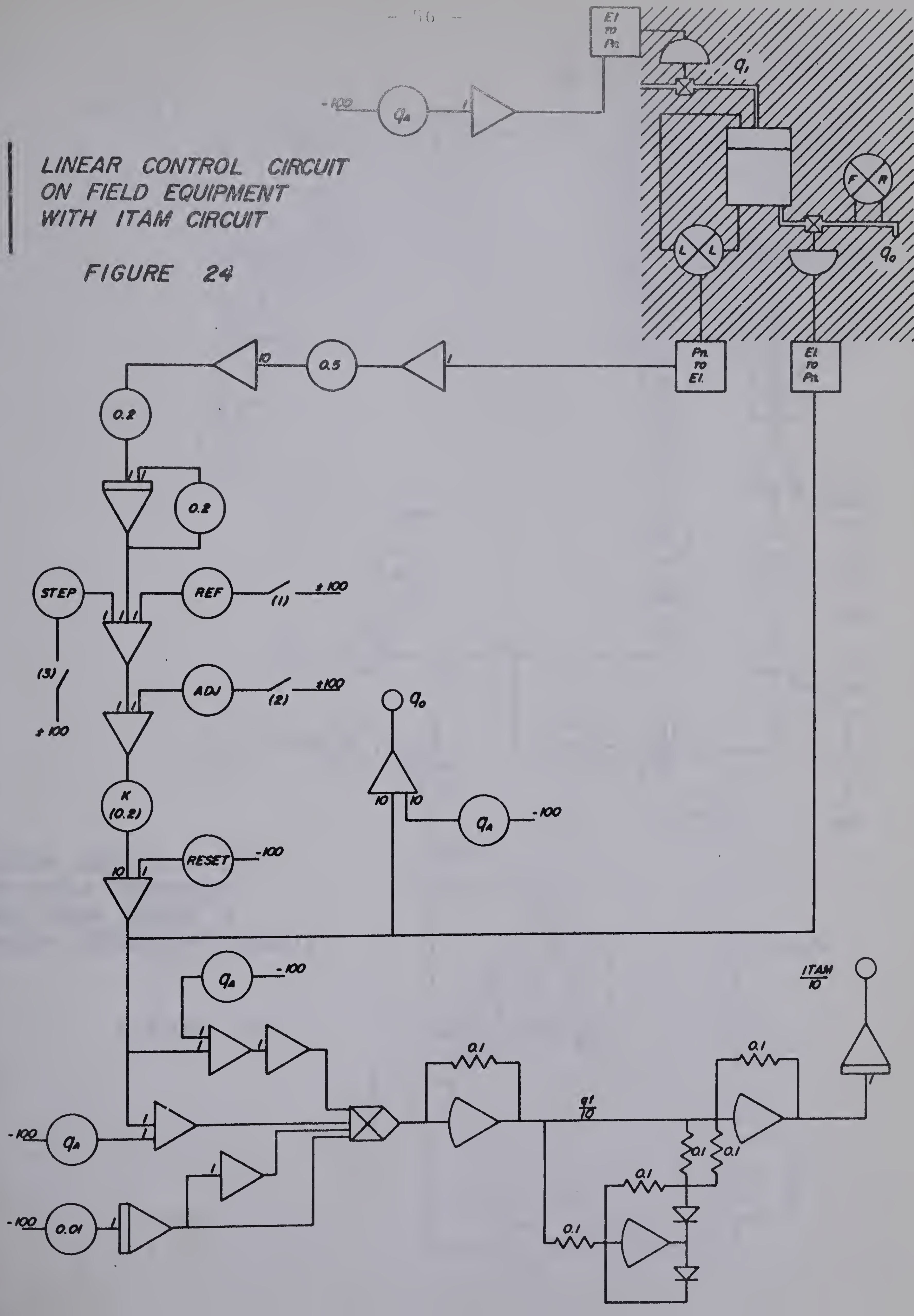

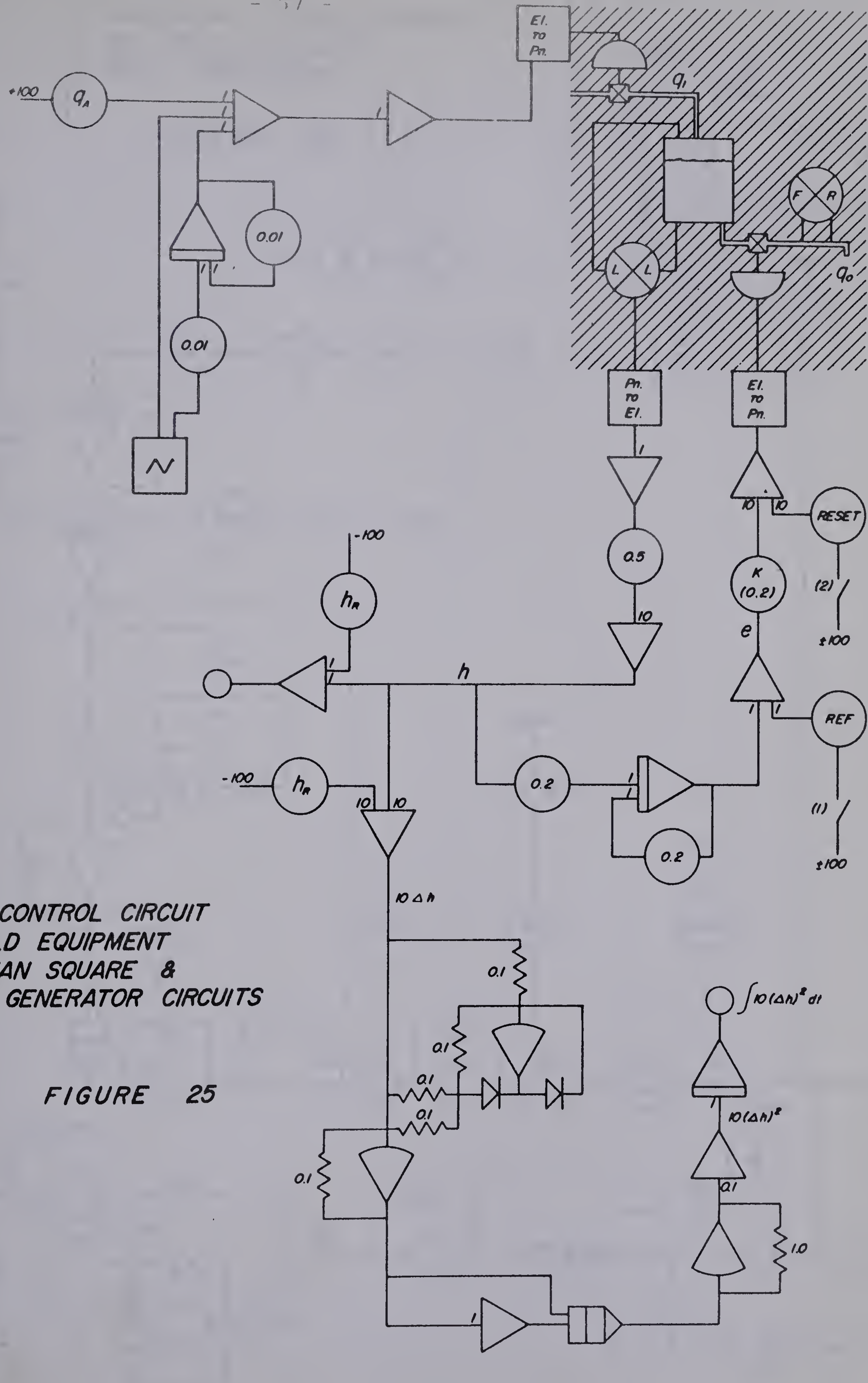

LINEAR CONTROL CIRCUIT
ON FIELD EQUIPMENT
WITH MEAN SQUARE &
RANDOM GENERATOR CIRCUITS

FIGURE 25

NONLINEAR CONTROL CIRCUIT
ON FIELD EQUIPMENT
WITH ITAM CIRCUIT

FIGURE 26

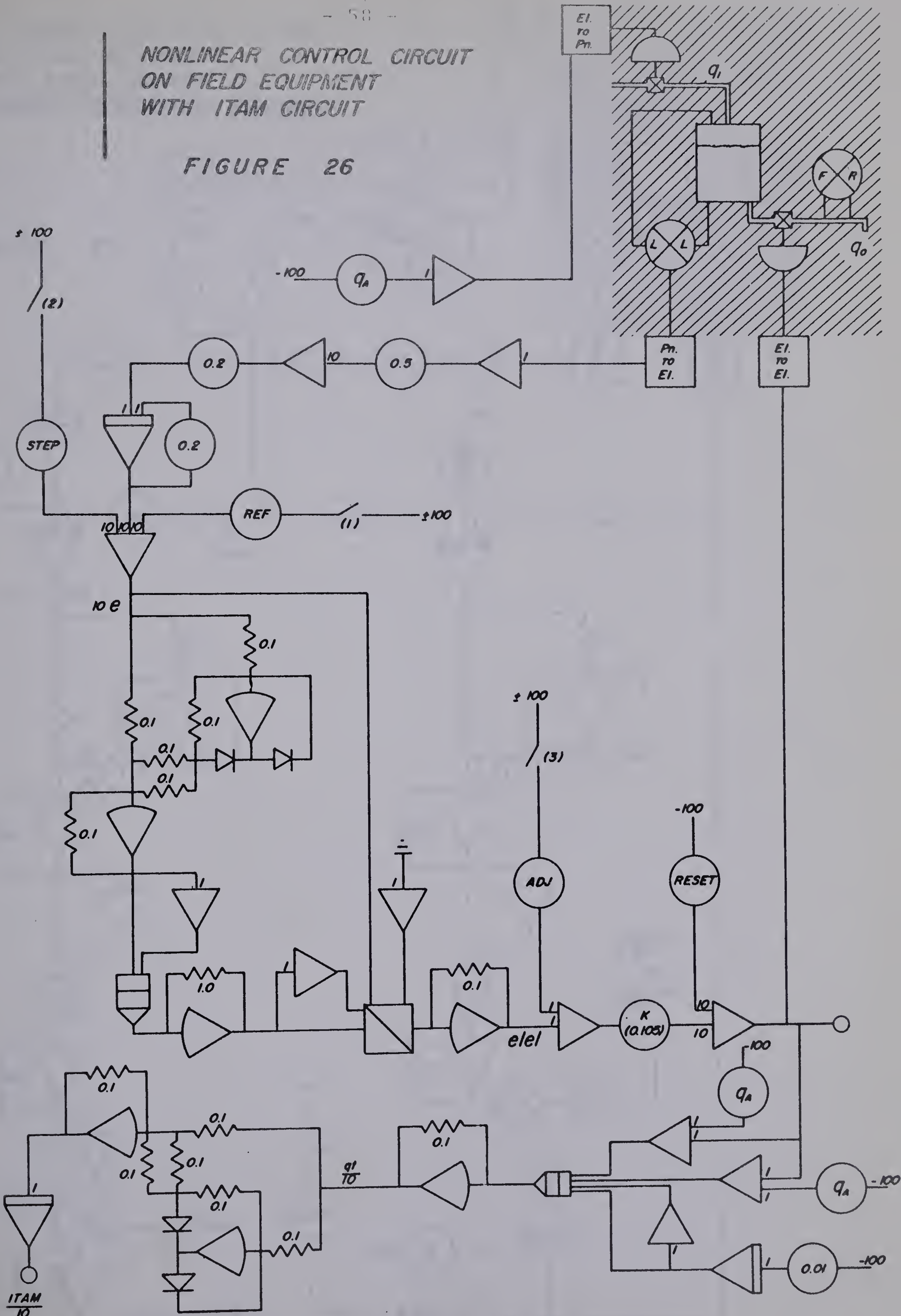

NONLINEAR CONTROL CIRCUIT ON FIELD EQUIPMENT WITH MEAN SQUARE & RANDOM GENERATOR CIRCUITS

FIGURE 27

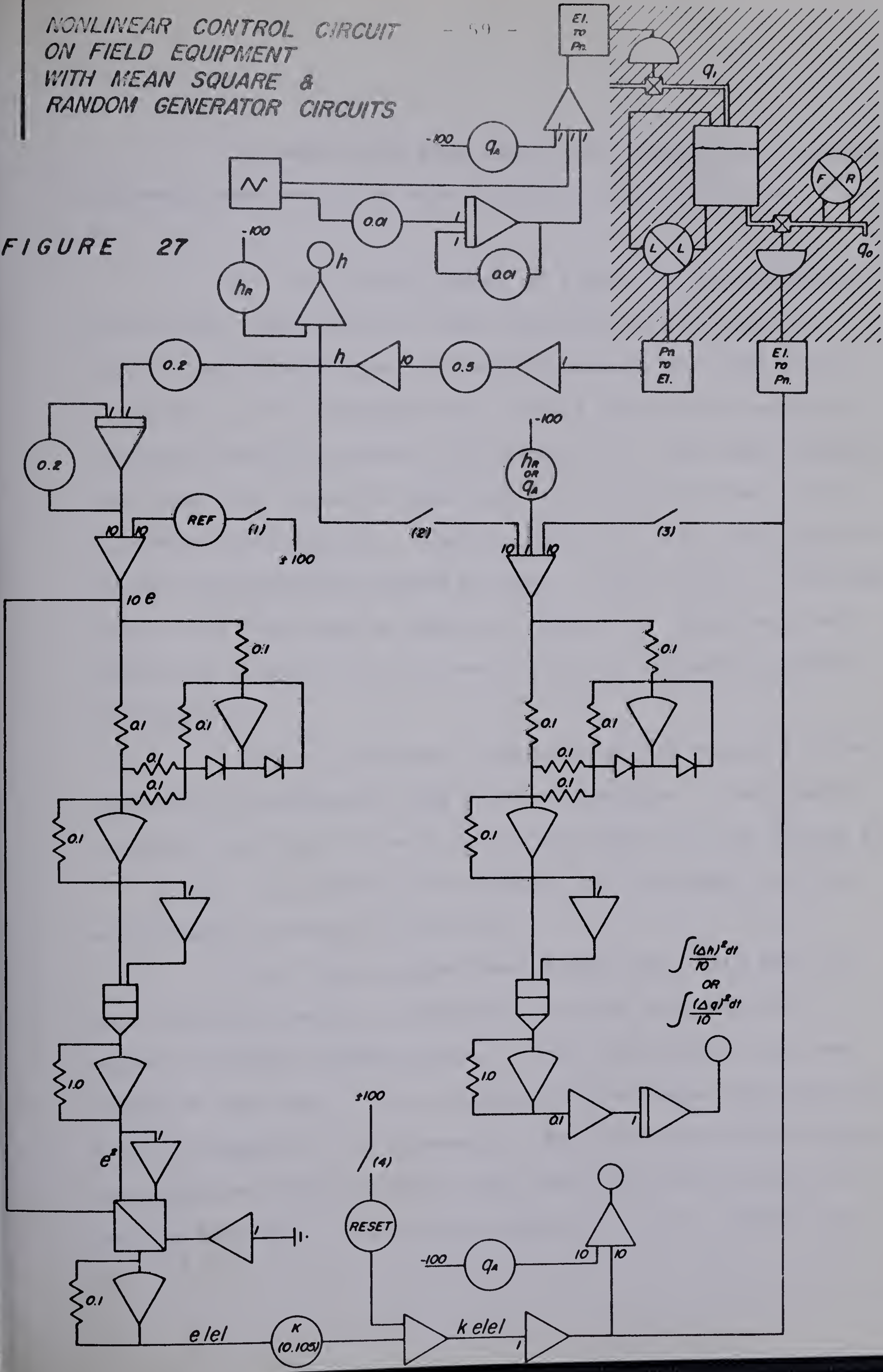

2) To obtain the ITAM values the computer and pneumatic equipment were set up as shown schematically in Figures 24 and 26.

For the linear system of Figure 24, the potentiometers were first fixed so that the tank was half full of water. The flow of water through the system was then set at 50 percent of its maximum value. (This was done by adjusting the potentiometers marked q_A on Figure 24.) The reset potentiometer was then adjusted until zero error was obtained. A 3-volt step was then set. Finally, the 3-volt step was applied and the potentiometer turned on that is set at 0.01. The ITAM values were then read as shown on Figure 24. This same procedure was repeated for different gains to collect the data for Figure 19.

For the nonlinear system, $e|e|$, of Figure 26, the procedure for obtaining ITAM data was the same. The results collected for the nonlinear system are also shown on Figure 19.

3) For obtaining rms values, the equipment was set up as shown on Figures 25 and 27.

The linear system (see Figure 25) again had its tank level and water flow adjusted so that they were 50 percent of their maximum values. Next the control loop was opened at the input to the feedback filter where the potentiometer is marked 0.2 on Figure 25. With this open loop circuit, the Gaussian random generator was adjusted until an h_{rms} of one was obtained. The gain was then set at 2.0. (This was

Figure 28. Comparison of q_o Under Linear and Nonlinear Control

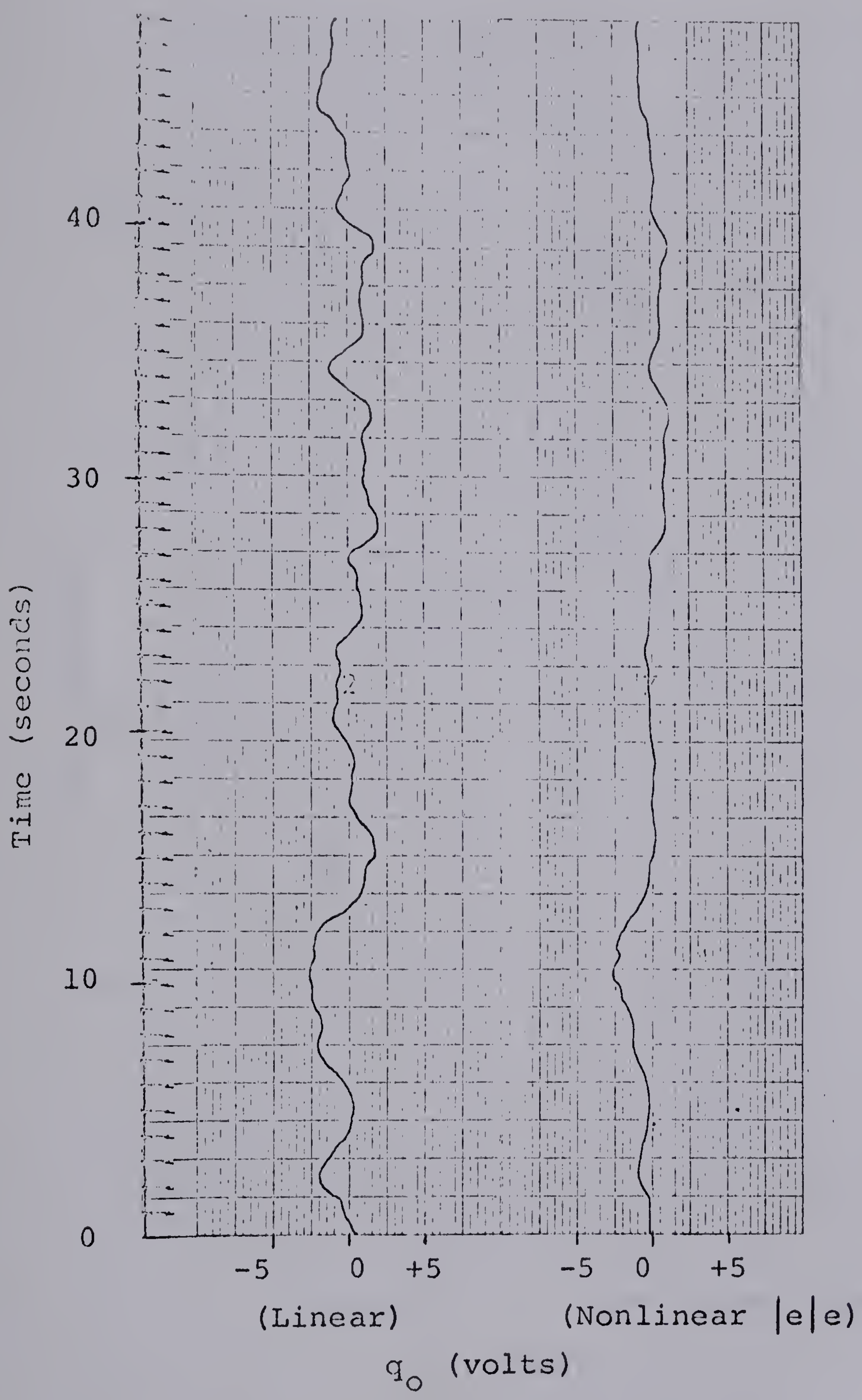

Figure 29. Comparison of h Under Linear and Nonlinear Control

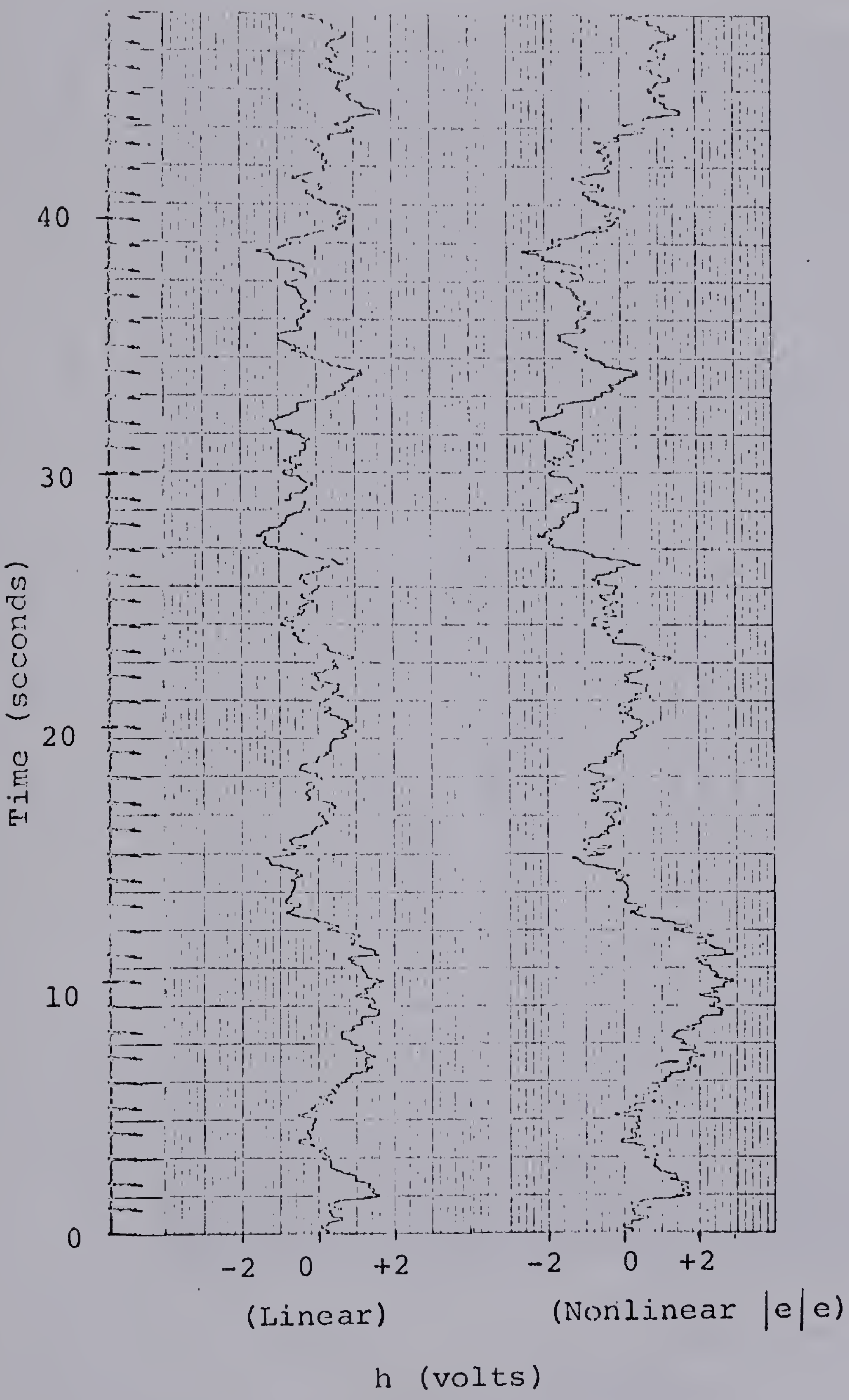

Figure 30. Comparison of q_o Under Linear and Nonlinear Control

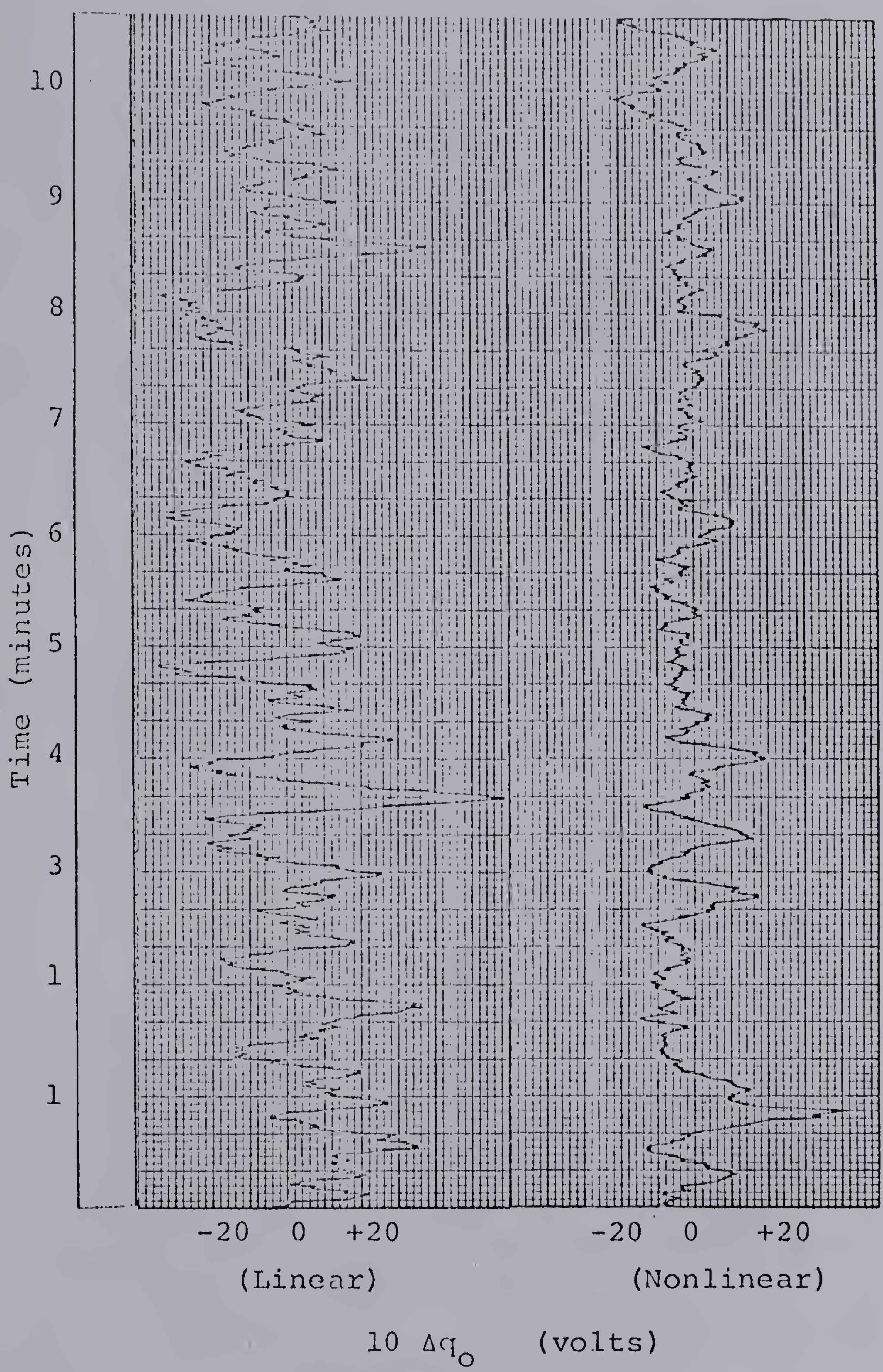

Figure 31. Comparison of $\dot{h}$ Under Linear and Nonlinear Control

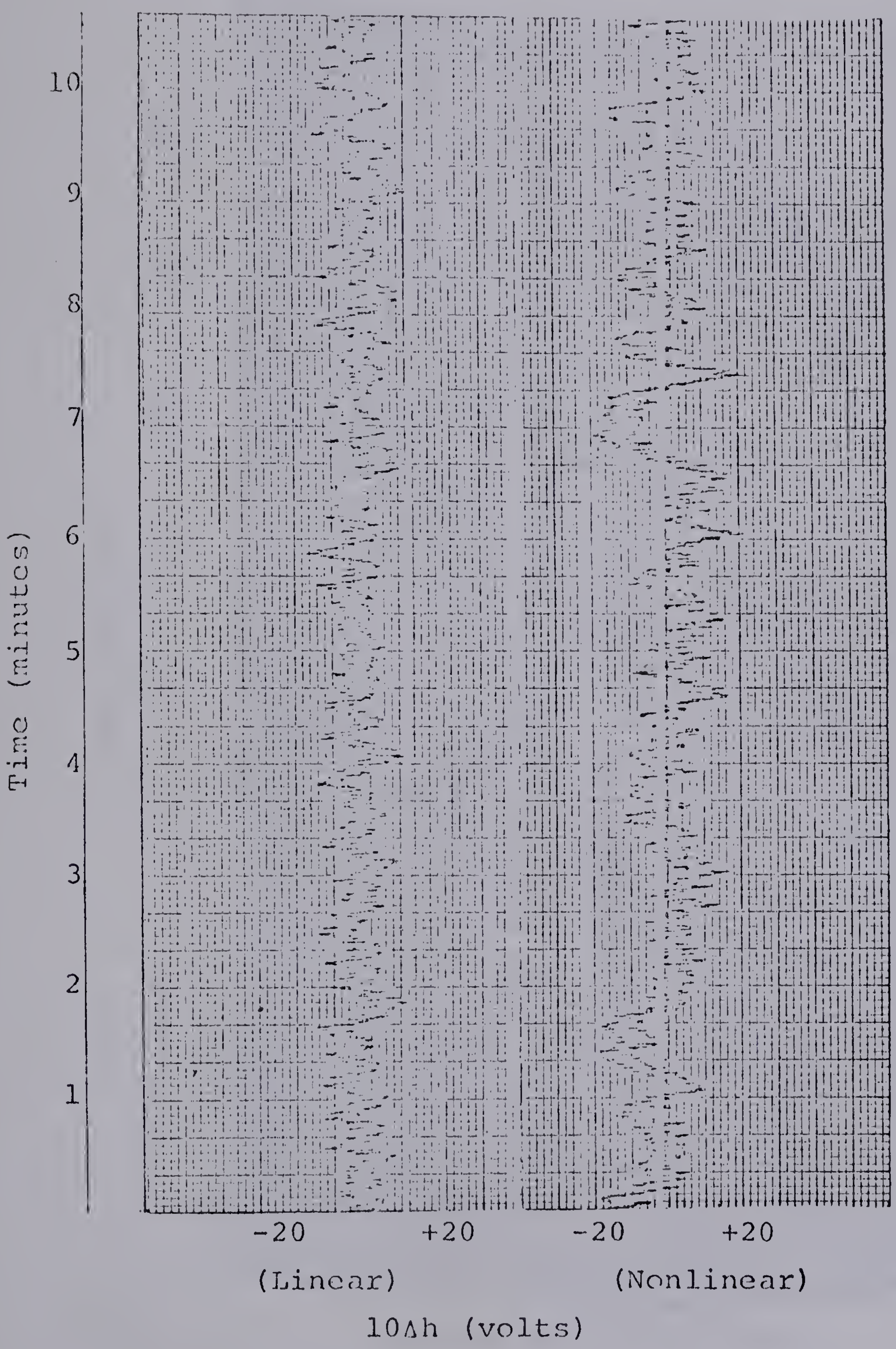

Figure 32. q_o Under Linear Control

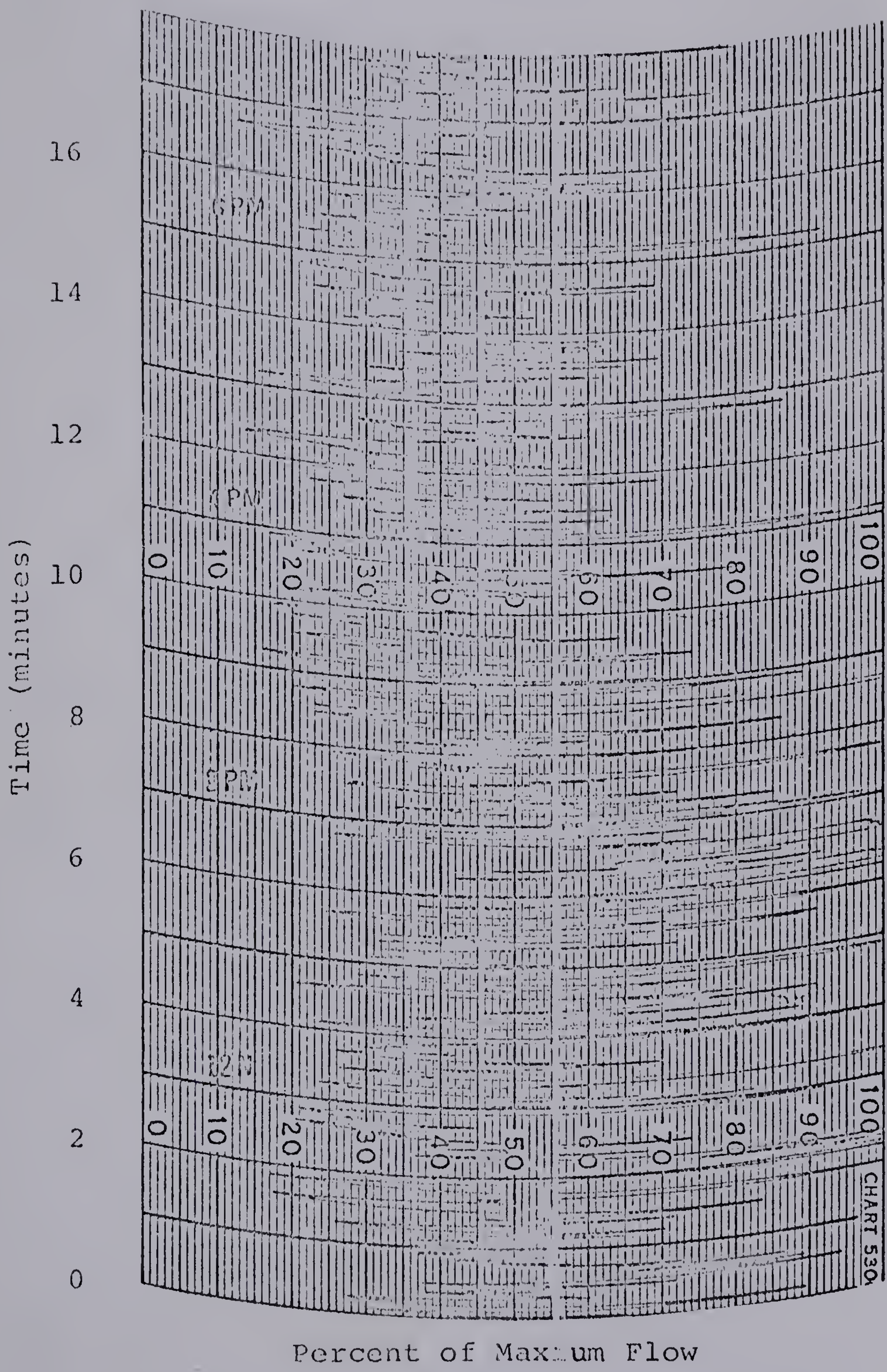

Figure 33. q_o Under Nonlinear Control

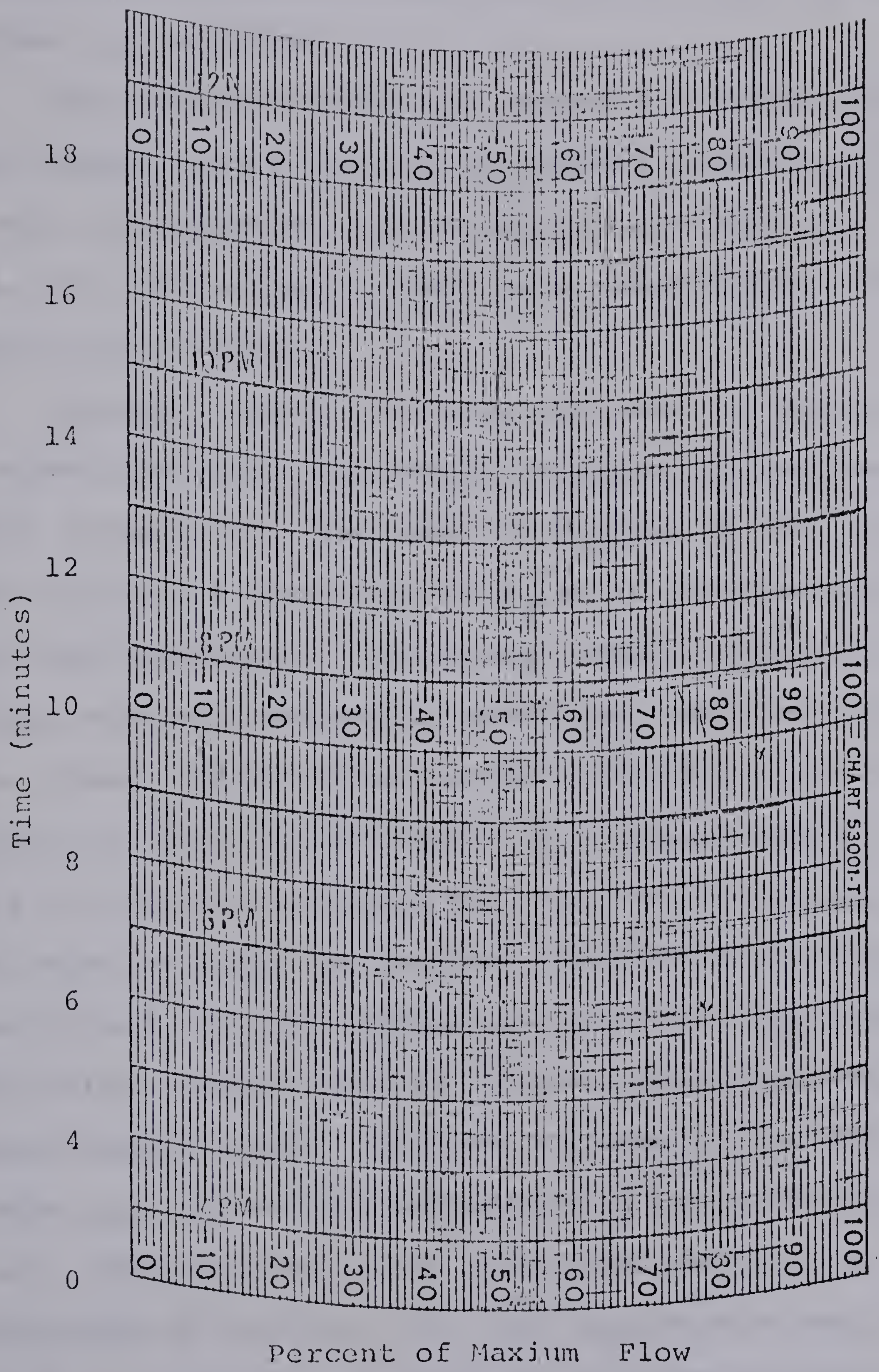

the gain that produced the lowest ITAM value for the linear system on Figure 19.) The control loop was connected again and the response of the controlled variable, h, and the manipulated variable, q_o, recorded.

The above procedure was repeated again for the nonlinear system, $e|e|$, with the components as shown on Figure 27. The only difference was that a gain of 1.05 was used. This was so the ITAM values matched, as on the computer model, at a step size of 3 volts.

Results - The ITAM values are shown on Figure 19. The recordings of the controlled variable, h, and the manipulated variable, q_o, are shown on Figures 30, 31, 32 and 33. Figure 30 shows a comparison of q_o as it was measured electrically before the transducer. (Note here, however, that all comparisons were not necessarily under the same load disturbance as the linear and nonlinear systems could not be run simultaneously on the field equipment as on the computer.) Figure 31 shows a comparison of h for the linear and nonlinear systems under the Gaussian random load fluctuations. Figure 32 and 33 taken together compare the linear and nonlinear values respectively of the manipulated variable, q_o, as measured pneumatically. The rms decrease in the manipulated variable, q_o, as measured pneumatically was approximately 35 percent. The increase in the controlled variable, h, was approximately 61 percent. The word approximate was used because the results change slightly if different sections of

the two runs with the linear and nonlinear systems are compared.

Conclusions and Discussion - The field equipment studies showed the same trends and approximate results as the theoretical work.

First, note how the ITAM curves from the computer studies and field equipment studies show essentially the same relationship between the linear curve and the nonlinear, $e|e|$, curve (see Figures 17 and 19). In both cases the curve for the nonlinearity, $e|e|$, as compared to the linear curve, is of a higher slope and reaches its lowest value at a smaller gain. However, one can also see that the actual values on the corresponding curves from the two different studies do not match in slope or gain. The nonlinear valve on the field equipment is the most likely reason why the above discrepancies occurred between the comparable curves on Figures 17 and 19.

Second, 11.5 percent was the largest percent error made in predicting rms changes. This occurred when the computer values predicted a 39 percent change in the manipulated variable, q_o, and the field equipment only produced a 35 percent change. The analytical results had predicted a 38 percent change and were thus out by a 9 percent error. This was the greatest deviation, also, of the analytical calculations from the field equipment results.

Although the fact that the suspected nonlinearity in the valve not taken into account in the theoretical study may have

contributed in large measure to the discrepancy between theoretical and experimental results and consequently detracted somewhat from the effectiveness of the mathematical model used. It must be pointed out that the theoretical study using the linear model did serve to narrow down the choice of controller for the system. To this extent then the model can be considered to be useful.

General Conclusions and Discussion

In this final section, the following topics are covered. First, a defense is given of the three criteria that guided the outcome of this study. Second, the reasons are presented for using a 3-volt step size to compare ITAM values and a Gaussian random generator setting that resulted in an open loop rms value of h equal to one for comparing all rms values. Third, problems with the experimental equipment are discussed. Fourth, the different types of control are re-examined. Finally, the author states why, in his judgement, the nonlinearity $e|e|$ is the best to use in the control loop of Figure 7.

The first criteria of this study, stability,is necessary for any controller. Without stability there is no control and, therefore, it is the most important criteria for any controller. The second criteria, ITAM, is important because industry wants start-up disturbances to damp out rapidly. This is because start-up disturbances are generally the worst a system has to undergo and industry does not want them to last long because of the problems they create with the rest of the down-stream processes. Since the manipulated variable, q_o, was the out-flowing stream in this study, ITAM describes the above desire mathematically. This criteria was placed second in preference because of the importance of start-up problems in industry. Industry also desires the controller

to move the manipulated variable only when necessary during actual operation. Again this is so that the downstream processes will be disturbed as little as possible. This desire is represented mathematically be demanding a low rms. (The average flow value is considered as zero and fluctuations from zero are used to calculate the rms value.)

A value of 3 volts as the comparison voltage for all ITAM values was chosen because the author felt that most start-up conditions would be such as to make the head change at start-up three times that of the open loop rms value of the head variation. This selection was quite arbitrary, however, and others may prefer some other value. The reason for using an open loop rms value of h equal to one was that this provided a definite standard. If a closed loop value were used the type of controller within the control loop would have played a part. The reason a given output from the Gaussian random generator was not used as a standard was because of the nonlinear valves. The author wanted to make certain the field equipment was undergoing approximately the same sort of load disturbance as the computer model. (Using the open loop value also aided the analytical calculation in that "n" for the Gaussian random generator was then easily calculated.)

The author had to tolerate two unknowns in this study because of the equipment used. First, the specifications supplied by the manufacturers of the Gaussian random generator indicated that the frequency band below 0.25 radions/sec was

uncertain. The manufacturers said they believed the band was flat to nearly 0.0 radions/sec. but they could not prove it. This is why the diagrams of Figures 16A, 16B and 16C are drawn with dashed lines below 0.25 radions/sec. Also, note on Figures 16B and 16C that the band widths from the Gaussian random generator fed to the computer and field equipment were not equal. Thus, the field equipment should suffer more from high frequencies. This was born out by the data of Figure 31. The second unknown the author had to tolerate was the fact that the linear and nonlinear systems could not be run simultaneously on the field equipment. Thus, one could not be certain that the load disturbances on both systems were alike. However, because fairly long runs were used to calculate the rms values, they are probably quite precise.

The nonlinearity $e|e|$ was chosen in this study, over higher powers such as e^3, for two reasons. One was because $e|e|$ has a longer range, than the higher powers, in which its ITAM value was better than the linear controller. Two, when the ITAM values of $e|e|$ were greater than the linear controller, the difference was not as great as that of the higher powers. Thus, the gain for the nonlinear controller, $e|e|$, was not as difficult to set to be in the valley just above the 3-volt step size on the curves shown on Figure 18. Also, as can be seen by the analytical calculations, the biggest change in rms is going from the linear system to the nonlinear system with $e|e|$. When one goes from $e|e|$ to

e^3, the change in the q_o rms is smaller than above and for the same change in the q_o rms value a greater percent increase in h_{rms} is required. The major disadvantage of the controller with the nonlinearity $e|e|$ was that its maximum h value was 35 percent higher than the linear controller's maximum h value. (This figure was obtained by considering all runs.) Because of this one might argue that the same effect as that given by the nonlinear controller, $e|e|$, could be obtained by lowering the gain on the linear controller so that its h_{rms} was 35 percent higher. Doing this, however, does not lower q_o rms the approximate 39 percent obtained with the nonlinear controller. Instead only an approximate 30 percent lowering of the rms of q_o is obtained and the ITAM value would be increased an approximate 110 percent. Thus, the start-up response would be greatly decreased in desirability and the manipulated variable would not be lowered as much as that by the nonlinear controller.

The author feels this study has contributed information in two aspects. First, it has designed a nonlinear controller that works well for the system described in this study. Also, information on stability, ITAM values and rms values have been given for the controlled system. Second, the study has shown how to use the statistical describing function method to calculate rms values. It has also extended the above method to include the manipulated variable, q_o.

The study verified the statistical describing function approach for analytical calculations to within 4.5 percent error on the computer model and to within 9 percent error on the field equipment.

In conclusion, the author would like to point out that $e|e|$ was chosen as the nonlinearity to use in this study because it fit the special specifications the best. However, should the demands on the controller change, there is little likelihood that $e|e|$ would be the answer as each special problem in nonlinear control theory demands a different type of function.

Bibliography

1. Brown, R.G. and Nilsson, J.W., Introduction to Linear Systems Analysis, John Wiley & Sons, Inc., N.Y., (1962).

2. Campbell, P.D., Process Dynamics, John Wiley & Sons, Inc., N.Y., (1958).

3. Eckman, D.P., Automatic Process Control, John Wiley & Sons, Inc., N.Y., (1958).

4. Gibson, J.E., Nonlinear Automatic Control, McGraw-Hill Book Co., Inc., N.Y. (1963).

5. Jackson, R., "Control Systems With Disturbances Satisfying Certain Bounding Conditions", The Theory of Optimal Control, Butterworths, London, (1963).

6. Skinners, S.M., Control System Design, John Wiley & Sons, Inc., N.Y., (1964).

7. Smith, O.J.M., Feedback Control Systems, McGraw-Hill Book Co., Inc., N.Y., (1958)

8. Technical Information, 29-113a, Gap-Action Floating Controller, The Foxboro Company, Foxboro, Mass., U.S.A.

9. Thaler, G.J. and Pastel, M.F., Analysis and Design of Nonlinear Feedback Control Systems, McGraw-Hill Book Co., Inc., N.Y., (1962).

FLOW CHART LEGEND

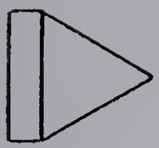	INTEGRATOR	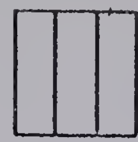	FUNCTION GENERATOR (PACE)
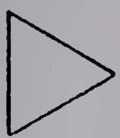	SUMMAR	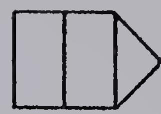	FUNCTION GENERATOR (APPLIED DYNAMICS)
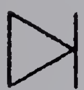	DIODE	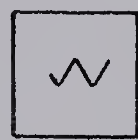	RANDOM GAUSSION GENERATOR
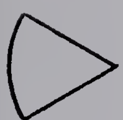	AMPLIFIER		PEN
	RESISTOR	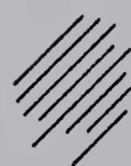	FIELD EQUIPMENT WITH PNEUMATIC CONTROL
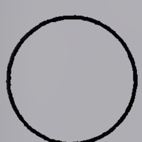	POTENTIOMETER	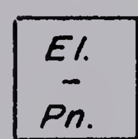	TRANSDUCER ELECTRIC TO PNEUMATIC
	SWITCH	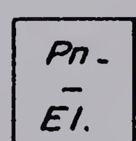	TRANSDUCER PNEUMATIC TO ELECTRIC
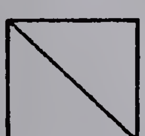	COMPARATOR & SWITCH		FLOW RECORDER (PNEUMATIC)
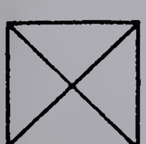	MULTIPLIER (PACE)	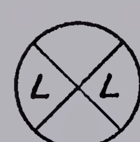	LIQUID LEVEL MEASURING ELEMENT
	MULTIPLIER (APPLIED DYNAMICS)	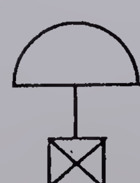	VALVE